frontiers in Earth Science

ORIGINAL RESEARCH
published: 18 November 2021
doi: 10.3389/feart.2021.745972

Reconstruction of Climate Changes Based $\delta^{18}O_{carb}$ on the Northeastern Tibetan Plateau: A 16.1-cal kyr BP Record From Hurleg Lake

Xueyun Ma[1,2], Zhifu Wei[1], Yongli Wang[3]*, Gen Wang[1], Ting Zhang[1], Wei He[1,2], Xiaoli Yu[1,2], He Ma[2,3], Pengyuan Zhang[2,3], Shangkun Li[1,2], Jingyi Wei[2,3] and Qiaohui Fan[1]*

[1]Key Laboratory of Petroleum Resources Research, Gansu Province, Northwest Institute of Eco-Environment and Resources, Chinese Academy of Sciences, Lanzhou, China, [2]College of Earth and Planetary Sciences, University of Chinese Academy of Sciences, Beijing, China, [3]CAS Center for Excellence in Life and Paleoenvironment, Key Laboratory of Cenozoic Geology and Environment, Institute of Geology and Geophysics, Chinese Academy of Sciences, Beijing, China

OPEN ACCESS

Edited by:
David K. Wright,
University of Oslo, Norway

Reviewed by:
Xianyong Cao,
Institute of Tibetan Plateau Research (CAS), China
Bernhard Aichner,
Leibniz-Institute of Freshwater Ecology and Inland Fisheries (IGB), Germany

***Correspondence:**
Zhifu Wei
weizf@lzb.ac.cn
Yongli Wang
ylwang@mail.iggcas.ac.cn

Specialty section:
This article was submitted to Quaternary Science, Geomorphology and Paleoenvironment, a section of the journal Frontiers in Earth Science

Received: *23 July 2021*
Accepted: *18 October 2021*
Published: *18 November 2021*

Citation:
Ma X, Wei Z, Wang Y, Wang G, Zhang T, He W, Yu X, Ma H, Zhang P, Li S, Wei J and Fan Q (2021) Reconstruction of Climate Changes Based $\delta^{18}O_{carb}$ on the Northeastern Tibetan Plateau: A 16.1-cal kyr BP Record From Hurleg Lake. Front. Earth Sci. 9:745972. doi: 10.3389/feart.2021.745972

Hydroclimate evolution history and changes in the Tibetan Plateau play significant roles in depicting paleoclimate and evaluating climatic conditions in the coming future. However, the interaction of the westerlies and the Asian monsoon complicates our understanding of the mechanism of climate variation over the Tibetan Plateau. In this study, we assessed the paleoclimate of Hurleg Lake, which was previously located in the convergence area of the East Asian monsoon and westerly wind. We first reconstructed the climatic conditions based on fined-grained authigenic carbonate $\delta^{18}O$ ($\delta^{18}O_{carb}$), plant-derived proxies of C/N, and *n*-alkane-derived $\delta^{13}C_{31}$. In the Hurleg Lake, $\delta^{18}O_{carb}$ was controlled by $\delta^{18}O$ changes of the lake water and evaporation. The climate evolution since ~16.1 cal kyr BP can be classified into three stages. The Lateglacial (16.1–11.0 cal kyr BP) was characterized by a warm-wet climate in the beginning, followed by a cold-dry climate since 12.0 cal kyr BP. Typical warm and cold phases occurred during 14.8–12.0 cal kyr BP and 12.0–11.1 cal kyr BP, which may correspond to the Bølling/Allerød (B/A) and Younger Dryas periods, respectively. The early to mid-Holocene was generally characterized by a warm-wet climate; however, notable cold-dry intervals occurred at ~8.3 cal kyr BP. The Late Holocene (after 4.8 cal kyr BP) displayed a significantly cold-wet climate. Finally, we examined the possible mechanisms responsible for the climate variability in the study area. The results showed that the long-term warm trend in the Lateglacial and colder trend after early Holocene was controlled by insolation. The Asian summer monsoon and the westerlies played a significant role in determining moisture sources during the Lateglacial. The East Asian monsoon contributed greatly to the moisture variation from the early to mid-Holocene, whereas the westerly winds dominated during the late Holocene. Combined, our findings highlight the complex changes in hydroclimate conditions since the last glacial in the Tibetan Plateau and provide crucial implications for comprehending the hydroclimate pattern in the transition zone of westerlies and Asian monsoon.

Keywords: carbonate isotopes, Asian monsoon, westerly, climate change, Tibetan Plateau

INTRODUCTION

Since the 21st century, global environmental problems, such as sea level rise, extreme climate events, and ecological environmental damage, have increased in frequency and intensity in response to global warming (Klanderud, 2005; IPCC, 2014). These climate events have adversely impacted human and social development and attracted the attention of researchers across the world (Haug et al., 2003; Mondoni et al., 2012). Scientifically predicting future climate change is necessary for tackling global climatic problems; however, the scale of modern meteorological records is too short to reliably evaluate and simulate future climate change laws. Moreover, past climate can inform future climate variability (Tierney et al., 2020); therefore, determining the history and forcing mechanisms of past climate is necessary for estimating future climate trends (Lunt et al., 2013; Chen et al., 2016; Tierney et al., 2020).

As many large rivers originate from the extensive alpine plateau and its adjacent mountains, the Tibetan Plateau (TP) supports rapidly growing societies with a population of 3 billion people or almost half of the world's population (Mischke and Zhang, 2010). Due to its role in social development and its susceptibility to climate change, the TP is a hotspot for studying climate variability. The TP is located in a climatic junction where the Asian monsoon and westerlies interact intensely. The region has high elevation (average elevation >4,000 m above sea level) and cold climatic conditions (mean annual air temperature <4°C) (Liu and Chen, 2000; Chen et al., 2016; Luo et al., 2019), and the ecological environment of the TP is more sensitive to climatic variability than most regions on Earth (Liu et al., 2009; Diffenbaugh et al., 2013). In addition, thousands of lakes are distributed across the TP, where paleoclimate information is well preserved. These include the hydroclimate and temperature records derived from lakes Naleng, Nam Co., Qinghai, Hurleg, Qionghai, etc. (Kramer et al., 2010; An et al., 2012; Zhao et al., 2013; Günther et al., 2015; Wang et al., 2020). Analyses of past climate changes have advanced our understanding of the dynamic driving factors of hydroclimate and temperature, which are closely related to the monsoon and insolation, respectively, and are influenced by regional and global climate changes (Peterse et al., 2004, 2011; Dykoski et al., 2005; Wang et al., 2005, 2008; Zhao et al., 2011).

Hurleg Lake lies on the northeastern Tibetan Plateau, at the intersection area, which was previously affected by both the East Asian monsoon and westerly wind (Winkler and Wang, 1993; Zhao et al., 2011). Due to the particularity of its geographical location and its climatic variability and sensitivity, many studies have reconstructed the Holocene climate based on the results of lake cores derived from Hurleg Lake, including paleotemperature, paleomoisture, and paleovegetation (Zhao et al., 2007, 2011; Zhao et al., 2010; Zhao et al., 2013; Fan et al., 2014; Rao et al., 2014; He et al., 2016; Song et al., 2020). However, these climatic records from Hurleg Lake mostly focused on the Holocene, while studies on the Lateglacial were limited. Moreover, the records were often conflicting, due to uncertainties in sediment chronologies, the climatic significance of the proxies used, the detailed evolutionary model of climate and environmental change reconstructed by various environmental indexes from the same core, or the same proxies derived from different cores (Chen et al., 2016). In Hurleg Lake, pollen-based reconstruction of paleoclimate patterns displayed a relatively wet climate in the earliest Holocene (11.9–9.5 cal kyr BP), followed by a dry climate during the mid-Holocene (9.5–5.5 cal kyr BP), while a stable and less dry climate occurred after 5.5 cal kyr BP (Zhao et al., 2007). The climate pattern was contradicted to most hydroclimate patterns on the northeastern Tibetan Plateau, such as the Qinghai Lake (Chen et al., 2016), Ximencuo Lake (Herzschuh et al., 2014), and Gahai Lake (Chen et al., 2007). What is more, Zhao et al. (2007) suggested that the position of the subtropical monsoon, the mid-latitude westerlies, and the local topography all contributed to the climate pattern in the Hurleg Lake area, while Zhao et al. (2010) found that the generally dry climate between 7.8 and 1.0 cal kyr BP could be correlated with decreases in East Asian and Indian monsoon intensities, and Fan et al. (2014) hold that the Westerlies and local topography rather than Asian summer monsoon dominate the moisture availability in this region during the Holocene. Thus, the climate pattern of the northeastern Tibetan Plateau remains unclear and controversial. These records also suggest the need for a denser network of sites to better clarify the spatially complex pattern of climate change and atmospheric circulation in this region.

Herein, we present a well-dated and multi-proxy paleoclimate record from a sediment core in Hurleg Lake (northeastern TP) covering ~16.1–~0.2 cal kyr BP, based on the characteristics of authigenic carbonate oxygen isotopes, organic indexes (C/N), and *n*-alkane-derived indexes. Combined with multi-proxies including previously published organic and inorganic geochemical indexes, we reconstruct the detailed climate evolution in the study area and discuss the forcing mechanisms. Our results provide more accurate scientific data and references for paleoclimate reconstruction to strengthen predictions of future climate evolution on the Tibetan Plateau.

STUDY AREA

Hurleg Lake (37°14′–37°20′ N, 96°51′–96°57′ E, elevation 2,817 m a.s.l) lies east of the Qaidam Basin, in the northeastern Tibetan Plateau (**Figure 1**). The lake covers an area of approximately 57.9 km^2, with an average water depth of 2.0 m and a maximum water depth of 9.6 m. The salinity of Hurleg Lake, which belongs to the freshwater lake of the sodium sulfate subtype, is about 1 g/l (Zhao et al., 2007). The Hurleg Lake region is outside the East Asian summer monsoon (EASM) edge currently and generally has a continental arid climate (Tian et al., 2001, 2003). The region is characterized by a large difference in the mean temperature between summer and winter, ranging from −9.7°C to 15.6°C, and the average annual temperature was about 4°C (1.6°C–5.2°C) over the past 48 years (1956–2004, Delingha climate station) (Yi et al., 1992). The annual precipitation is approximately 160 mm, and annual evaporation is ca. 2,000 mm (Yi et al., 1992; Zhao et al., 2013). The water in Hurleg Lake is mainly recharged by surface runoff, from the Bayin River and Barogen River, which both eventually flow into Toson Lake through a small stream (Wang

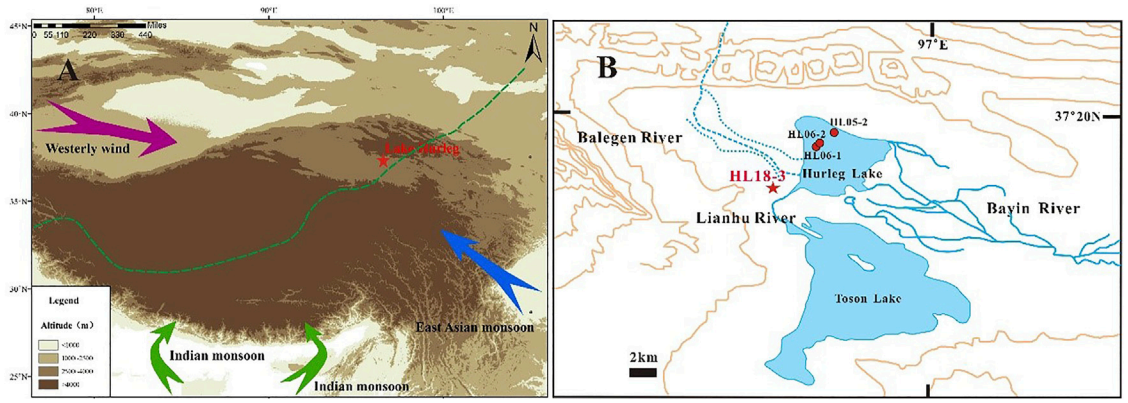

FIGURE 1 | Location of the study area. **(A)** Map showing the study site of Hurleg Lake (red pentagram); the purple, green, and blue arrows indicate westerly wind, Indian monsoon, and East Asian monsoon, respectively; the modern East Asian monsoon limit is shown by the green dashed line (after Gao, 1962; and Chen et al., 2008). **(B)** Core locations of HL18-3 (this study, red solid Pentagram), HL05-2, HL06-1, and HL06-2 (red solid circles) (Zhao et al., 2010).

and Dou, 1998; Zhao et al., 2010, 2011). Located in the temperate desert zone, the main vegetation in the lake area is desert grassland (gravel desert) and desert shrub (vial desert) (Zhou et al., 1990). The coastal area of the lake is surrounded by a large portion of marsh vegetation including common reeds (*Phragmites communis*), *Hippuris* spp., and *Scirpus* spp., (Zhao et al., 2007).

MATERIALS AND METHODS

Coring and Age Model

A 520-cm-long sediment core named HL18-3 (37°15′10.91″N, 96°51′06.06″E) was recovered in a wetland at the southwest edge of Hurleg Lake (**Figure 1**) using portable soil sampling rig in July 2018. The sediment core was wrapping up by aluminum foil paper and preserved by a plastic tube. The HL18-3 core lithology is composed of yellowish-brown silt (0–171 cm), pale yellow mud (171–285 cm), gray–white silt mingled with plant residues (285–383 cm), light gray mud (383–448 cm), dark gray silt (448–505 cm), and gray–white silt (505–520 cm) (**Figure 2**), sequentially.

Six sediment organic matter samples and two plants residue samples derived from the HL18-3 core (**Table 1**) were collected for accelerator mass spectrometry (AMS) ^{14}C dating (Ma et al., 2021). The ^{14}C age was calibrated with the IntCAL13 curve (Reimer et al., 2013), and then the calibrated ^{14}C ages were used to reconstruct the age-depth model in the R software package bacon v.2.3.7 (**Figure 2**) (Blaauw and Christen, 2011; Blaauw et al., 2020). Considering the "old carbon" effect, the upper 3.5-m core was analyzed through the method of geomagnetic relative paleointensity (RPI). Before the RPI test, the rock magnetic and environmental magnetic experiments were conducted. Using NRM30mT/SIRM30mT as the index of RPI change, the upper 167 cm generally conforms to the established criteria for RPI reconstruction (Ma X. et al., 2021). By matching our RPI results with published RPI records, three credible RPI ages were gotten in the upper 167 cm of the HL18-3 core (**Table 1**) (Ma et al., 2021). The AMS ^{14}C ages were determined on the AMS at the Beta Analytic, Miami, USA. The magnetic experiments were carried out in the Palaeomagnetism and Geochronology Laboratory of the Institute of Geology and Geophysics, Chinese Academy of Sciences. Data of AMS ^{14}C ages as well as the rock magnetic and environmental magnetic were published on the journal "Quaternary Geochronology" (Ma et al., 2021).

Authigenic Carbonates

The analyses of δ^{13}C and δ^{18}O of carbonates were conducted on the gas stable isotope mass spectrometer (Thermo Scientific Delta V—GasBench II, Thermo Fisher Scientific, Waltham, MA, USA). Prior to measurement, plant residues and microbiological shells were picked out under a magnifying glass. After that, each sample was sieved less than 200 mesh. The treated sediment samples were loaded into glass vials and placed in an aluminum heating block of GasBench II; samples (~0.1 g) were purged by helium for 7 min, followed by treating with supersaturated phosphoric acid (98%) for 2 h, and the reaction temperature is 72°C. Ultimately the CO_2 generated by the reaction was carried into the Delta V by helium for detection. The international reference material is NBS-18, the national reference material is GBW04405, and the delta values are reported in per mil relative to the Vienna Pee Dee Belemnite (VPDB), with error less than 0.1‰.

Organic Proxies

The organic elements were determined by a vario MICRO cube (Elementar Company, Langenselbold, Germany). After combustion, the sample was further catalyzed and C and N elements were converted into detectable gases within a redox process. Pure oxygen was introduced into the system to support combustion. After combustion, the sample was further catalyzed and redox catalyzed, in which C and N elements were all converted into various detectable gases. After further separation by a chromatographic column, these gases were finally analyzed by the detector.

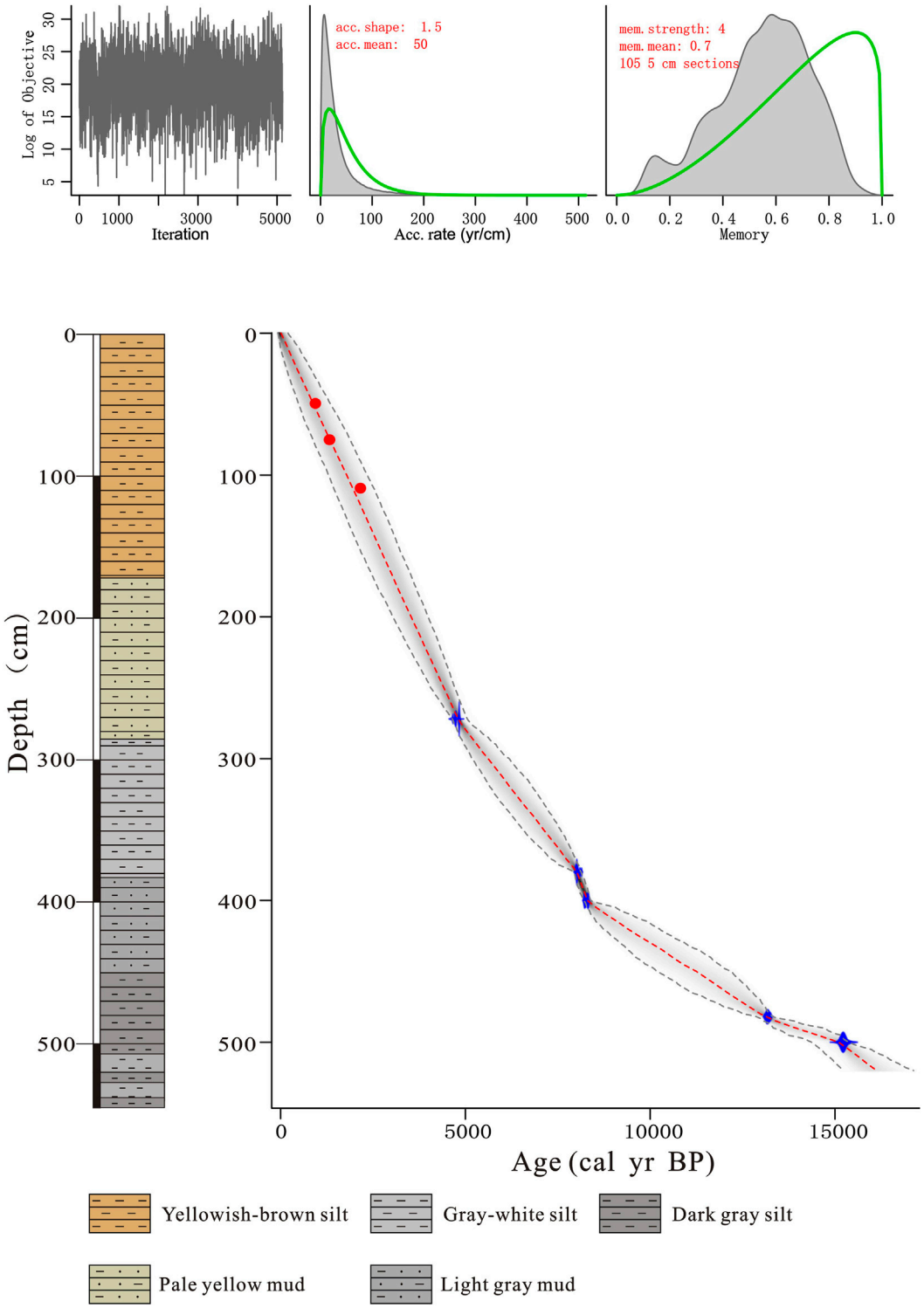

FIGURE 2 | Age-depth model of the HL18-3 core based on bacon. The red solid circles are the RPI age, the blue marks are AMS ^{14}C ages dated by organic matter, and the green mark is AMS ^{14}C age dated by plant remains; the shaded part between the gray dotted lines represents the error interval.

X-ray Diffraction Method

The X-ray diffraction (XRD) experiment was conducted on Ultima IV. Samples were crushed to <200 mesh in an agate mortar, and then the powder sample was loaded into the aluminum circular sample tank with the sample spoon. Finally, the sample was transferred into the instrument for

TABLE 1 | AMS^{14}C radiocarbon dates and RPI age from the HL18-3 core in the northeastern TP.

Lab code	Depth (cm)	AMS^{14}C age ± error (yr BP)	Calibrated age ± error (yr BP)	Material
Beta-500846	9	2,490 ± 30	2,730–2,460	Organic sediment
Beta-500847	50	3,500 ± 30	3,855–3,692	Organic sediment
Beta-498158	272	4,230 ± 30	4,857–4,806	Organic sediment
Beta- 586690	380	7,400 ± 30	8,334–8,170	Plant residues
Beta-500849	380	7,220 ± 30	8,067–7,965	Organic sediment
Beta-527480	400	7,460 ± 30	8,413–8,201	Plant residues
Beta-498157	482	11,340 ± 40	13,279–13,093	Organic sediment
Beta-500851	500	12,780 ± 40	15,385–15,082	Organic sediment
Lab code	Depth (cm)	RPI age	Material	
HL-49	50	1,000	Soil sediment	
HL-75	75	1,400	Soil sediment	
HL-109	110	2,200	Soil sediment	

TABLE 2 | Component of fine-grain carbonate evaluated by the XRD method of the HL18-3 core.

Sample	Depth (cm)	Calcite (%)	Dolomite (%)	Aragonite (%)	Gypsum (%)	(Calcite + aragonite)/carbonate (%)
HL-0	0	84.62	13.12	0.00	2.26	84.62
HL-8	8	74.04	15.38	0.00	10.58	74.04
HL-40	40	86.29	13.71	0.00	0.00	86.29
HL-108	108	78.26	10.63	0.00	11.11	78.26
HL-150	150	75.90	12.31	0.00	11.79	75.90
HL-200	200	71.21	7.78	21.01	0.00	92.22
HL-248	248	18.48	12.38	69.13	0.00	87.62
HL-300	300	50.66	15.28	29.69	4.37	80.35
HL-348	348	48.43	20.47	31.10	0.00	79.53
HL-396	396	35.47	21.28	43.24	0.00	78.72
HL-440	440	17.38	18.81	63.81	0.00	81.19
HL-500	500	76.85	9.72	13.43	0.00	90.28
Average	—	51.93	14.50	30.78	2.79	82.42

testing. The scanning mode was 2 theta/theta goniometer; the sample level does not move. The technical indexes of the instrument were as follows: scanning range, 0.5–159°; minimum step, 0.0001°; angle reproducibility <0.0001°.

RESULTS

A total of 12 samples were collected at intervals of ~50 cm for the analysis of the XRD results to determine the mineral types. The main carbonate mineral is calcite, ranging from 17.4% to 86.3%, with an average value of 52% (n = 12). The total percentage of calcite and aragonite varied from 74.0% to 92.2%, with an average value of 82.4% (n = 12). Other minerals, such as dolomite and gypsum, are rare (**Table 2**).

A total of 65 subsamples were collected at 8-cm intervals from the HL18-3 core and analyzed on the Delta V (Thermo Scientific). The values of $\delta^{13}C_{carb}$ ranged from −2.29% to 5.19‰, with an average value of 1.88‰ (n = 65), and those of $\delta^{18}O_{carb}$ ranged from −8.39% to −1.52‰, averaging −5.16‰ (n = 65) (**Table 3**). $\delta^{13}C_{carb}$ displayed a generally positive trend during the Lateglacial and became negatively correlated with fluctuation from Early to Late Holocene (**Figure 5A**).

C/N ratios were generally utilized to distinguish organic matter derived from various sources. In the HL18-3 core, 64 samples were analyzed for C and N elements (**Table 3**), and the C/N ratios varied from 29.3 to 0.1, with an average value of 12.7 (n = 64). The C/N ratios were relatively high during the early to mid-Holocene, while an uptrend occurred in the Lateglacial and displayed a decreased tendency in the late Holocene interval (**Figure 5A**).

DISCUSSION

Age-Depth Model

Using linear extrapolation, the calculated RPI age at 9 cm of the core was 160 cal yr BP, and that at 50 cm of the core was 1,000 cal yr BP; the corresponding AMS ^{14}C ages were 2,595 cal yr BP and 3,773 cal yr BP, respectively. Thus, the "old carbon" reservoir ages at 9 and 50 cm were 2,435 cal yr BP and 2,773 cal yr BP, respectively, which is close to the reservoir age (2,758 cal yr BP) of core HL06-2 from Hurleg Lake (Zhao et al., 2009; Zhao et al., 2010).

However, owing to the spatiotemporal variability of the carbon reservoir, the carbon reservoir could differ between the sediment

TABLE 3 | $\delta^{18}O_{carb}$ of fine-grain carbonate and C/N ratios of the HL18-3 core.

Sample	Depth (cm)	$\delta^{18}O_{carb}$ (PDB, ‰)	C/N	Sample	Depth (cm)	$\delta^{18}O_{carb}$ (PDB, ‰)	C/N
HL-0	8	−6.02	7.24	HL-33	272	−2.95	20.43
HL-1	16	−6.79	5.76	HL-34	280	−3.00	21.60
HL-2	24	−6.10	6.16	HL-35	288	−3.50	17.54
HL-3	32	−5.99	6.11	HL-36	296	−4.02	21.72
HL-4	40	−5.66	0.13	HL-37	304	−3.93	19.88
HL-5	48	−6.65	0.11	HL-38	312	−3.56	19.06
HL-6	56	−7.34	0.33	HL-39	320	−4.90	25.08
HL-7	64	−7.84	0.27	HL-40	328	−5.31	12.56
HL-8	72	−7.86	0.36	HL-41	336	−4.27	10.50
HL-9	80	−8.39	14.45	HL-42	344	−4.10	10.37
HL-10	88	−7.99	10.83	HL-43	352	−4.50	12.70
HL-11	96	−7.16	0.12	HL-44	360	−5.16	0.10
HL-12	104	−6.72	0.12	HL-45	368	−4.84	14.82
HL-13	112	−7.40	0.25	HL-46	376	−5.27	15.70
HL-14	120	−7.75	10.81	HL-47	384	−5.75	12.78
HL-15	128	−6.93	0.10	HL-48	392	−4.20	17.15
HL-16	136	−7.39	18.68	HL-49	400	−3.32	10.39
HL-17	144	−6.90	20.27	HL-50	408	−2.68	14.45
HL-18	152	−6.17	14.41	HL-51	416	−1.99	11.72
HL-19	160	−6.86	14.08	HL-52	424	−3.37	15.60
HL-20	168	−6.02	11.17	HL-53	432	−3.68	13.09
HL-21	176	−6.42	17.39	HL-54	440	−2.03	16.37
HL-22	184	−6.95	19.35	HL-55	448	−1.52	19.59
HL-23	192	−5.42	21.08	HL-56	456	−2.76	15.73
HL-24	200	−5.50	14.73	HL-57	464	−4.09	11.35
HL-25	208	−5.95	19.10	HL-58	472	−3.37	20.15
HL-26	216	−4.70	20.36	HL-59	480	−3.14	9.38
HL-27	224	−5.34	29.14	HL-60	488	−3.20	10.74
HL-28	232	−4.64	24.73	HL-61	496	−2.22	0.06
HL-29	240	−5.36	29.27	HL-62	504	−6.36	0.12
HL-30	248	−3.43	21.08	HL-63	512	−7.74	0.05
HL-31	256	−3.72	17.16	HL-64	520	−5.49	—
HL-32	264	−5.52	18.13	Average	—	−5.16	12.72

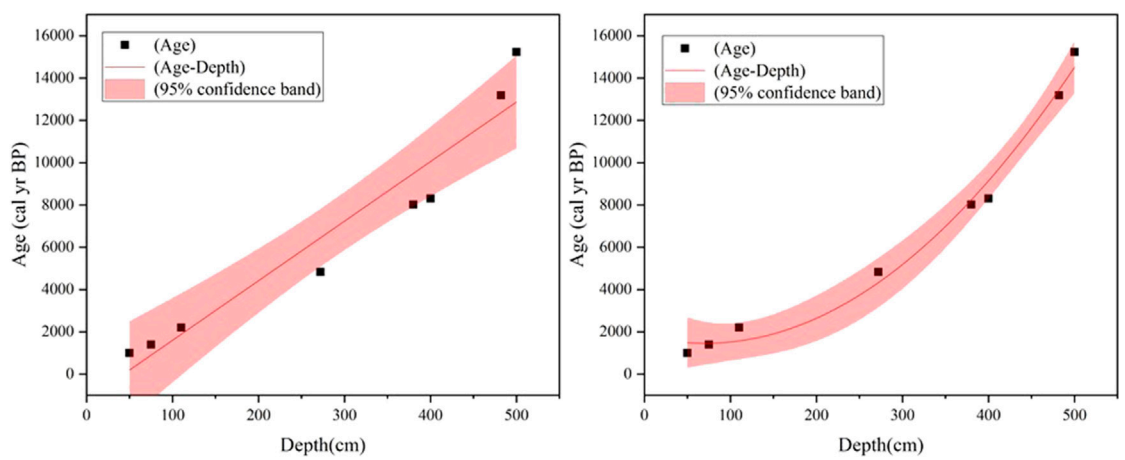

FIGURE 3 | Relationship between ages and depths in the HL18-3 core. The former is the linear relationship and the latter is the quadratic regression relationship.

cores from the same area (Reimer and Reimer, 2006; Mischke et al., 2013; An et al., 2012; Zhou et al., 2014). Moreover, the carbon reservoirs within the same core are not always constant (Schneider et al., 2019; Soulet et al., 2019), and the commonly used method of subtracting the carbon reservoir ages from the whole section may be unreasonable. Nevertheless, the occurrence of a linear relationship or a quadratic regression suggests that the carbon reservoirs are constant because the hydrochemical conditions in the lake are generally stable (Xiao et al., 2004; Herzschuh et al., 2006; An et al., 2012; Zhang et al., 2016).

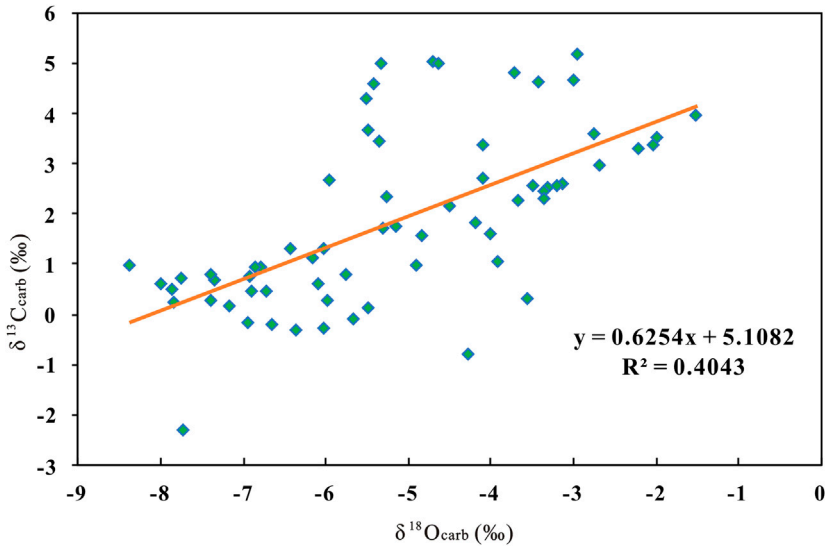

FIGURE 4 | Correlation between $\delta^{18}O_{carb}$ and $\delta^{13}C_{carb}$ in the HL18-3 core.

According to the analysis of the relationship between ages (including three RPI ages in the upper 110 cm and five AMS^{14}C ages under 110 cm) and depths, we obtained a significant linear relationship (R^2 = 0.93, p < 0.001, n = 8) and quadratic regression (R^2 = 0.99, p < 0.001, n = 8) (**Figure 3**). Three ages obtained by the geomagnetic RPI method are reliable and not affected by the reservoirs. The linear and quadratic regression relationship suggests that there is little or no carbon reservoir effect below 110 cm (Ma et al., 2021). To support this finding, the radiocarbon dating of plant remains in a sample at 380 cm returned a date practically identical to that dated by the organic matter at the same depth (**Table 1**).

Origin of Carbonates

Previous studies have shown that the carbonate in lake sediments with grain sizes less than 200–300 mesh is authigenic carbonate (Jiang and Wu, 2003; Zhang et al., 2016). In order to minimize the possible effect of exogenous carbonate, samples <200 mesh were selected for testing carbonate isotopes. In addition, the XRD results displayed that calcite was the dominated carbonate mineral, with the calcite and aragonite contents accounting for 82.3% of the total carbonate. In contract, the contents of dolomite and gypsum are relatively low (**Table 2**). Moreover, we found no large exposed carbonatite in the study area. Consequently, fine-grained carbonates can represent lake authigenic carbonate.

Furthermore, several studies have reported positive or negative correlations between $\delta^{18}O_{carb}$ and $\delta^{13}C_{carb}$. Talbot and Livingstone (1989) and Talbot (1990) found that $\delta^{18}O_{carb}$ was positively correlated with $\delta^{13}C_{carb}$ across a large number of lakes in central Asian and Africa; they also identified a stronger correlation with longer water retention time but no correlation in open lakes. In addition, Leng and Marshall (2004) revealed that $\delta^{18}O_{carb}$ correlated positively with $\delta^{13}C_{carb}$ in the sediment of freshwater and saltwater lakes, but not in groundwater recharge lakes. The positive correlation between $\delta^{13}C_{carb}$ and $\delta^{18}O_{carb}$ in the lakes of northwestern China reported by Zhang et al. (2016) indicated a closed lake, with a long retention time and obvious salinization characteristics. The $\delta^{18}O_{carb}$ and $\delta^{13}C_{carb}$ results of carbonate in the HL18-3 core showed consistent variability patterns, exhibiting a positive correlation (**Figure 4**, n = 65, R^2 = 0.4071, p < 0.001). The Hurleg Lake is a freshwater lake in which the sodium sulfate subtype is about 1 g/l (Zhao et al., 2007). Although Hurleg Lake is currently an open freshwater lake, its salinity was generally higher in the past (**Figure 6E**) (He et al., 2016). In addition, according to the annual total river inflow and lake volume, the mean residence time of the Hurleg Lake is approximately 1 year (Zhao et al., 2010).

The variability in carbonate content under different water depths at Hurleg Lake was found to be controlled by the dilution of endogenic carbonate by fine-grained silicates delivered from surrounding deserts with sparse vegetation cover (Zhao et al., 2010). Thus, the change in the carbonate percentages was used to reflect the variation in water depth. Prior to the study, Zhao et al. (2010) observed a flash flood event in 2005, in which a large amount of alluvial sediment was transported from the area west of the lake. However, more detrital material was deposited in shallow water because the dense vegetation covering the lake bottom trapped the materials in the littoral zone. Similarly, the inflowing rivers are surrounded by dense marshes, and river channels are unlikely to transport clastics into the lake (Zhao et al., 2010). The HL18-3 core is located in the southwestern part of the lake, where it is far away from the river mouth (**Figure 1B**). Although exogenous clastic minerals might have an effect on sedimentary carbonate, the effect is likely to be slight. Accordingly, we suggest that the fine-grained carbonate in Hurleg Lake is mainly derived from authigenic carbonates, and the variabilities of carbonate $\delta^{18}O_{carb}$ are capable of indicating the climate change in the study area.

Implications of Climatic Proxies

Climatic Implications of $\delta^{18}O_{carb}$

The carbonate $\delta^{18}O_{carb}$ values in lake sediments are generally controlled by the $\delta^{18}O$ of lake water, water temperature, and disequilibrium effects (Bowen, 1990; Gasse et al., 1991; Yu and Eicher, 1998; Leng and Marshall, 2004). Tian et al. (2003) analyzed the $\delta^{18}O$ of modern precipitation water derived from the Delingha, where it is nearby the Hurleg Lake; the results revealed a strong temperature influence on precipitation isotopic composition in the Qaidam Basin, with higher temperature corresponding to higher isotopic value in precipitation. However, water temperature affects the $\delta^{18}O$ fractionation from lake water into carbonate, which could induce an equilibrium fractionation coefficient of −0.25‰ per °C during calcification (Epstein et al., 1953). The changes in $\delta^{18}O$ values of the HL18-3 core sediments reached 6.87‰, which led to an approximately 27.5°C temperature difference, and there is no evidence for such a high-amplitude change. Therefore, the variabilities of $\delta^{18}O_{carb}$ cannot account for the variation in the water temperature.

The disequilibrium effects were proven to be negligible at Gengahai Lake on the northeastern Tibetan Plateau (Qiang et al., 2017) and were rarely discussed when evaluating the paleoclimate. Therefore, the $\delta^{18}O_{carb}$ records of the Hurleg Lake could have been controlled primarily by variations in the $\delta^{18}O$ of lake water ($\delta^{18}O_{Lw}$). There is another fact that largely parallel first-order variations in the $\delta^{18}O$ values derived from various carbonate species suggest that all the $\delta^{18}O$ records provide a reasonable approximation of lake water $\delta^{18}O$ (Apolinarska and Hammarlund, 2009; Clegg and Hu, 2010; Qiang et al., 2017). In Hurleg Lake, water samples have an average $\delta^{18}O$ value of −4.9‰ (n = 15) (He et al., 2016); besides, water isotope measurements of 13 samples taken from Hurleg Lake between 2004 and 2007 have a range from −6.6% to −3.3‰ for $\delta^{18}O$ (Zhao et al., 2010). The average value of $\delta^{18}O_{carb}$ in the HL18-3 core is −5.16‰ (n = 65) (**Table 3**), and the average value of $\delta^{18}O_{carb}$ from the upper 50 cm of the HL18-3 core is −6.20‰ (n = 6); the $\delta^{18}O_{carb}$ values are similar to the $\delta^{18}O$ in the lake water. Therefore, it is considered that the changes in $\delta^{18}O_{carb}$ can represent the variation of $\delta^{18}O$ in lake water. Hence, factors contributing to $\delta^{18}O_{Lw}$ will in turn affect the composition of $\delta^{18}O_{carb}$. Among these factors, the $\delta^{18}O$ values of the regional rainfall and lake hydrology are the most significant ones (Zhang et al., 2011). Meteorological data from the Delingha weather station show that the lake area of Hurleg Lake was significantly correlated with the annual runoff of the Bayin River (R = 0.78), while the latter is closely related to the mean annual precipitation (Fu et al., 2008; Fan et al., 2014). On the other hand, compared to the annual runoff of the Bayin River, meteorological analyses show that melting ice and snow from glaciers are in low proportion (Fu et al., 2008; Fan et al., 2014). Therefore, the lake area and lake level of Hurleg Lake are dominated by the annual precipitation of the lake catchment (Fan et al., 2014). Correspondingly, the variations in moisture sources and precipitation amounts were considered as significant controls on $\delta^{18}O_{carb}$.

In general, moisture transported by the Westerly wind to the region is much more ^{18}O-depleted than that from the summer monsoon (Araguás-Araguás et al., 1998; Tian et al., 2007 ; ; Zhang et al., 2011). Hurleg Lake is located in the transition zone of Westerly wind and Asian monsoon in the past (Winkler and Wang, 1993; Zhao et al., 2011); the variation of moisture source has excellent potential for affecting $\delta^{18}O$ in precipitation. Besides, there is a negative correlation arising from the "amount effect," whereby the heaviest rainfall is most depleted in $\delta^{18}O$ (Dansgaard, 1964; Zhang et al., 2011). In the monsoon region, significant correlations between $\delta^{18}O$ of precipitation and rainfall amount were observed from the meteorological station (Johnson and Ingram, 2004; Dayem et al., 2010). Although the precipitation amount in the Hurleg Lake region now is low, in the past, the precipitation amounts probably are in large value. This is due to the elevation of three palaeoshorelines in the Holocene which are ~4, ~7, and ~9 m above the present lake level (Fan et al., 2014), and there was a mega-paleolake during the early Pleistocene to late Pleistocene (~2,800–2,700 m a.l.s) in the north-eastern Qaidam Basin (Huang and Cai, 1987). Thereby, the rainfall amounts could also contribute to the variabilities of $\delta^{18}O$ in precipitation, in turn affecting $\delta^{18}O_{carb}$ in lake sediments.

In dryland regions, for closed lakes, the water loss is dominated by the evaporation; $\delta^{18}O_{Lw}$ is therefore strongly influenced by the precipitation/evaporation (P/E) ratio. In previous studies, variations in the $\delta^{18}O_{carb}$ of lake sediments derived from arid to semiarid regions have always been interpreted as reflecting the balance between regional precipitation and evaporation (P/E) (Lister et al., 1991; Wei and Gasse, 1999; Liu et al., 2007; Zhang et al., 2011). In south Tibet, Tian et al. (2008) suggested that the $\delta^{18}O_{Lw}$ values in several closed lakes are very sensitive to relative humidity. However, the Hurleg Lake is an open lake, the rapid discharge of a lake system always reduces the lake water residence time and thus decreases the effect of evaporation on $\delta^{18}O_{Lw}$ (Develle et al., 2010). The Donggi Cona Lake in the Tibetan Plateau provided good evidence, due to the $\delta^{18}O_{carb}$ values becoming more negative after ~4.0 cal kyr BP, when the lake became hydrologically open (Mischke and Zhang., 2010). Nevertheless, a recent study on isotopes of Hurleg Lake water displayed that the $\delta^{18}O$ values suffered from a cumulative evaporation effect in which it became stronger from source water to hydrologically open lakes (e.g., Hurleg Lake), then to closed lake systems (He et al., 2016). Further, the results of ^{2}H and ^{18}O derived from Hurleg Lake water samples fall on a local evaporation line, indicating that the lake water isotopes were influenced by evaporation (He et al., 2016). Therefore, it seems that the impact of evaporation on open lakes cannot be ignored.

Overall, the shifts of $\delta^{18}O_{carb}$ values from negative to more positive in the Hurleg Lake region over the episodes since the Lateglacial can be interpreted primarily as a decrease in the amounts of precipitation coupled with an increase in the regional P/E ratios, indicating the decrease in regional effective precipitation (Zhang et al., 2011) and representing a dryer climate. Besides, the changes in the moisture source between

westerly wind and Asian monsoon may also have played a dramatic role in controlling the $\delta^{18}O_{carb}$ values.

Climatic Implications of Organic Proxies

Organic matter in the lake sediments originating from terrestrial higher plants contains a large number of nitrogen-free biomacromolecules, such as lignin, cellulose, and hemicellulose, which are characterized by carbon enrichment. In contrast, aquatic plants, such as phytoplankton, are characterized by nitrogen enrichment because they are rich in proteins and other substances (Meyers, 1994b; Meyers, 1997; Hedges, et al., 1997). Therefore, the C/N ratio can be utilized to distinguish organic matter derived from various sources, where the C/N ratio ranges of 4–10, 10–20, and >20 correspond to aquatic plants or algae, submerged/phytoplankton or mixed sources of terrestrial and emergent plants, and terrestrial higher plants, respectively (Meyers, 1994b; Jia and Peng, 2003; Hu et al., 2009).

Atmospheric CO_2 exists in three isotopic forms ($^{12}CO_2$, $^{13}CO_2$, and $^{14}CO_2$); owing to the different activities of light and heavy isotopes in thermal gradients or biochemical reactions, carbon isotope fractionation occurs in plants during transpiration and biosynthesis. The mean $\delta^{13}C_{TOC}$ value for C_3 plants is −27‰ (range from −33‰ to −22‰), and for C_4 it is −13‰ (range, −16–9‰) (Cerling et al., 1997). For individual leaf wax *n*-alkanes, $\delta^{13}C$ values are ~6‰–8‰ lower than for bulk tissues (Rieley et al., 1993; Huang et al., 2001); thus, the variabilities of individual leaf wax *n*-alkanes can reflect changes in C_3 and C_4 plants. C_4 plants prefer to grow in areas with sufficient sunshine, higher temperatures, and drier conditions, primarily composed of warm and dry grassland vegetation (Edwards and Smith, 2010; Strömberg, 2011). C_4 plants have a higher water-use efficiency than C_3 plants and enriched in $\delta^{13}C_{31}$ (Edwards and Smith, 2010; Strömberg, 2011). Several recent studies suggested that submerged aquatic plants with enriched $\delta^{13}C$ may contribute to the concentrations of long-chain *n*-alkanes (nC_{27}, nC_{29}), while nC_{31} is a reliable proxy for estimating the variabilities of C_4 plants (Liu and Yang, 2015; Liu and Liu, 2016). Thus, $\delta^{13}C_{31}$ was used to reconstruct the evolutionary history of C_4 vegetation (Ma et al., submitted for publication). Generally, higher $\delta^{13}C_{31}$ suggests an expansion of C_4 plants, corresponding to a warmer climate.

Climate Changes on the Northeastern Tibetan Plateau Since the Lateglacial

Lateglacial (Ca. 16.1–11.1 cal kyr BP)

The generally enriched $\delta^{18}O_{carb}$ value of fine-grained carbonates suggested a decreased effective precipitation and thus a dryer climate during this period (**Figure 5A**). However, during this period, the fluctuating upward trend of mean annual precipitation in the Ximencuo Lake northeastern TP coincided with a wetter climatic condition (**Figure 7E**) (Herzschuh et al., 2014), and the depleted $\delta^{18}O$ of stalagmite calcite from Dongge Cave indicates a strong intensity of Asian monsoon (Dykoski et al., 2005). In addition, the increased C/N ratio revealed that the contribution of terrestrial higher plants to sediments increased (**Figure 5B**), and the C_4 plants expanded as indicated by more positive $\delta^{13}C_{31}$ values (**Figure 5C**). These results indicated a flourishing of terrestrial and aquatic plants, corresponding to a warm-wet climatic environment. Typically, moisture transported by the summer monsoon to the Tibetan Plateau is more $\delta^{18}O$-enriched than that of the westerly wind, because of the higher condensation temperature and/or weaker "rain-out" after a shorter air-mass transport distance (Araguás-Araguás et al., 1998; Tian et al., 2007; Qiang et al., 2017). In addition, the $\delta^{18}O$ values of fresh snow samples derived from the Qaidam Basin in January 2000 ranged from −29.4‰ to 20.8‰ (average of −26.2‰), which is significantly more negative than that of Hurleg Lake water (Qiang, 2002; Zhao et al., 2010). Furthermore, a previous study on the northeastern Tibetan Plateau revealed that the hydroclimate was controlled by monsoon-derived, westerly derived, and/or locally recycled moisture in several durations of the Lateglacial (Qiang et al., 2017). Henderson et al. (2010) attributed the depleted $\delta^{18}O_{carb}$ during the Little Ice Age at Lake Qinghai to the enhanced input of westerly wind. Considering the rapid discharge of the Hurleg Lake system, the $\delta^{18}O$ of lake water was significantly correlated with the annual runoff of Bayin River (R = 0.78), (Fu et al., 2008; Fan et al., 2014). The dramatic hydro-variation of the $\delta^{18}O$ signal induced by the transformation of westerly wind and monsoon would be recorded by the $\delta^{18}O_{carb}$ at Hurleg Lake. Therefore, the positive shift in $\delta^{18}O_{carb}$ during 16.1–14.8 cal kyr BP in the Hurleg Lake may be dominated by the strengthened monsoon, and after ~14.8 cal kyr BP, $\delta^{18}O_{carb}$ represents multiple changes in monsoon intensity (**Figure 5A**). The $\delta^{18}O_{carb}$ derived from the lake sediments in the adjacent areas of Geanggahai Lake in the Qaidam Basin, northeastern Tibetan Plateau, displayed a similar tendency with that of Hurleg Lake (**Figure 7B**). Combined with other evidence derived from Geanggahai Lake, the data suggest that the Asian summer monsoon may start to dominate the study region at ~15.3 cal kyr BP (Qiang et al., 2017).

Accordingly, the depleted $\delta^{18}O_{carb}$ indicated a wet climate from ~14.8 to ~12.0 cal kyr BP and enriched $\delta^{18}O_{carb}$ values during 12.0–11.1 cal kyr BP (**Figure 5A**), indicating a switch to a drier climate. These findings are in good agreement with the climate reconstructions interpreted by C/N and $\delta^{13}C_{31}$ (**Figure 5B**). The wet-warm conditions at 14.8–12.0 cal kyr BP were likely a response to the wet-warm Bølling/Allerød (B/A) event in the northeast Atlantic Ocean (Bard et al., 2000). At that time, pollen records from Lake Ximencuo on the northeastern Tibetan Plateau inferred that a Cyperaceae-rich high alpine meadow replaced the dry glacial flora at ~15.5 cal kyr BP, which was then further replaced by alpine meadow and shrubland at 14.0–12.5 cal kyr BP, indicating a humid climate (Herzschuh et al., 2014). The corresponding pollen-based mean annual temperature and precipitation showed a gradual increasing trend in 15.5–12.5 cal kyr BP and showed lower values during 12.5–10.8 cal kyr BP (**Figures 7D,E**) (Herzschuh et al., 2014). In addition, the U^K_{37} record at Lake Qinghai inferred a significantly increase in temperature since 15.1 cal kyr BP, which remained at relatively high temperature until 12.6 cal kyr BP. This

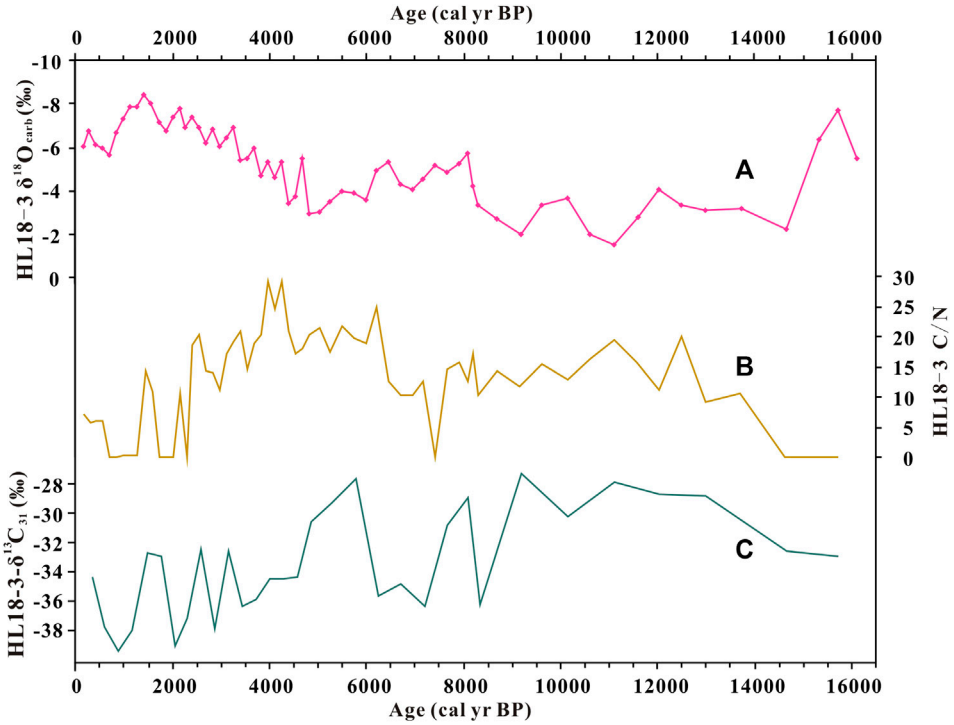

FIGURE 5 | Climate proxies derived from the HL18-3 core. **(A)** The $\delta^{18}O_{carb}$ in the HL18-3 core. **(B)** The C/N ratios in the HL18-3 core. **(C)** The n-alkanes derived $\delta\ ^{13}C_{31}$ in the HL18-3 core.

was followed by a lower temperature during 12.6–11.7 cal kyr BP (**Figure 7C**) (Hou et al., 2016).

After that, the 12.0–11.1-cal kyr BP dry interval at the Hurleg Lake may be linked to the Younger Dryas period (Shakun and Carlson, 2010), which markedly affected most regions of the Northern Hemisphere, including the Tibetan Plateau. Lake Dongxiong Co. in the southwestern Tibetan Plateau experienced a 3.8°C drop in temperature during 12.3–11.4 cal kyr BP (Ling et al., 2017). Other lake records on the Tibetan Plateau, such as Qinghai Lake (Ji et al., 2005), Lake Sumxi Co. (Gasse et al., 1991), and Lake Nam Co. (Günther et al., 2015), revealed a commonly cold-dry/wet climate lasting from ~12.9 to ~10.0 cal kyr BP.

Early to Mid-Holocene (Ca. 11.1–4.8 cal kyr BP)

Soon after 11.1 cal kyr BP, the $\delta^{18}O_{carb}$ values rapidly decreased and reached a relatively low value at ~10 cal kyr BP and then increased (**Figure 5A**), inferring a wet climate in the early Holocene, which may be induced by the enhanced Asian monsoon (**Figure 8E**) (Dykoski et al., 2005). Since ~8.3 cal kyr BP, $\delta^{18}O_{carb}$ quickly depleted and then gradually enriched, reflecting a wetter climate than the previous stage, and a drier climate in the late mid-Holocene (**Figure 6A**). During this interval, the $\delta^{13}C_{31}$ values were generally high in 11.1–9.2 cal kyr BP and then decreased to low values during 9.2–8.3 cal kyr BP. This corresponds to a warm climate at the beginning of the Holocene, which was interrupted by a cold interval around 8.3 cal kyr BP (**Figure 5C**). The ~8.3-cal kyr BP cold event has been commonly acknowledged in large numbers of studies on the Tibetan Plateau (Herzschuh et al., 2006, 2014; Mischke and Zhang, 2010; Zhang and Mischke, 2009) and in the Hurleg Lake (Zhao et al., 2007; Zhao et al., 2010; Zhao et al., 2013; He et al., 2016). The precipitated carbonate $\delta^{18}O$ of the HL05-2 core showed a similar variation trend to the $\delta^{18}O_{carb}$ in the HL18-3 core during 9.2–8.3 cal kyr BP (**Figure 6B**), which signified a dry climate (Zhao et al., 2010). Moreover, the lake level reflected by the carbonate content suggested that of the lake contracted notably at ~7.9 cal kyr BP (**Figure 6C**) (Zhao et al., 2010). The reconstructed salinity *via* alkenone-based $\%C_{37:4}$ exhibited relatively high values at 7.7–8.2 cal kyr BP (**Figure 6E**), indicating a dry climate (He et al., 2016). Besides, $U^{k'}_{37}$-derived ΔT fluctuated rapidly at low values during this period, which then increased distinctly after ~8.0 cal kyr BP (**Figure 6D**) (Zhao et al., 2013). Furthermore, pollen concentrations were low during intervals (**Figure 6F**) (Zhao et al., 2007; Zhao et al., 2013), and the C_4 plant indicator was significantly reduced (**Figure 5C**, Ma et al., submitted for publication); correspondingly, the organic matter percentage declined during 8.3–8.7 cal kyr BP (**Figure 6G**) (Zhao et al., 2010). When considering chronological errors, we determined the occurrence of a vital cold-dry event, which may be related to the frequently recorded 8.2-cal kyr BP cold event in the North Atlantic and many parts of the world (Johnsen et al., 1992; Alley et al., 1997; Thomas et al., 2007; Hede et al., 2010).

The enriched $\delta^{13}C_{31}$ value after ~8.3 cal kyr BP indicates a recovery of C_4 plants (**Figure 5C**). From ~8.0 to ~6.2 cal kyr BP, the low $\delta^{18}O_{carb}$ value suggested a generally wet climate, corresponding to a high lake level, reported by Fan et al.

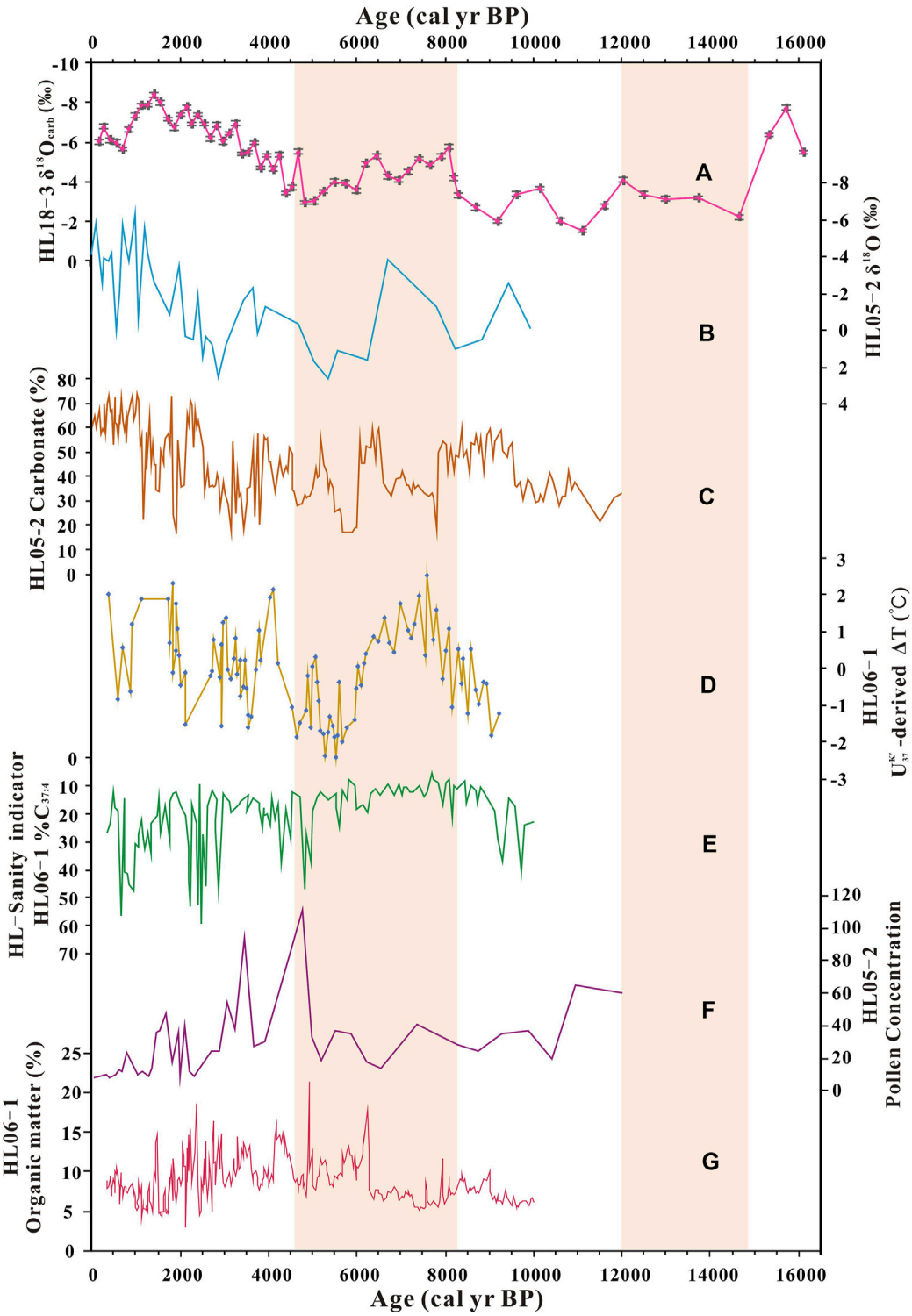

FIGURE 6 | Multiple geochemistry-proxy records derived from Hurleg Lake. **(A)** The $\delta^{18}O_{carb}$ in the HL18-3 core. **(B)** The $\delta^{18}O_{carb}$ in the HL05-2 core (Zhao et al., 2010). **(C)** The carbonate percentage (%) of the HL05-2 (Zhao et al., 2010). **(D)** $U^{K'}_{37}$-derived temperature record (ΔT) from the HL06-1 core (Zhao et al., 2013). **(E)** Salinity indicator of alkenone-based $\%C_{37:4}$ derived from HL06-1 (He et al., 2016). **(F)** Pollen concentration from HL05-2 (Zhao et al., 2007; Zhao et al., 2013, with updated chronology). **(G)** Organic matter percentage (%) of HL06-1 (Zhao et al., 2010).

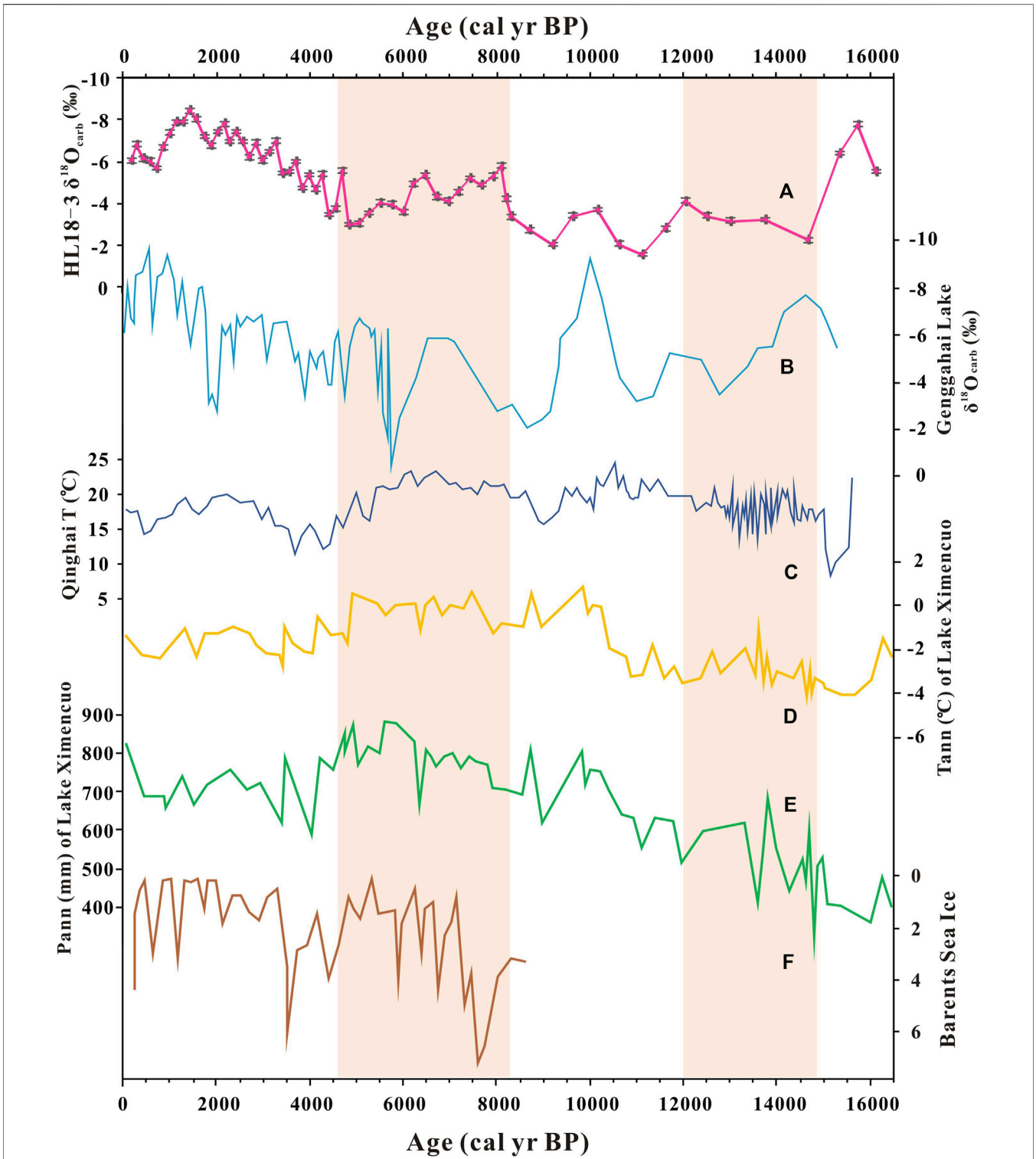

FIGURE 7 | Comparison of regional climate records. **(A)** The $\delta^{18}O_{carb}$ in the HL18-3 core. **(B)** The $\delta^{18}O_{carb}$ Genggahai Lake core (Qiang et al., 2017). **(C)** U^{K}_{37} inferred temperature record at Lake Qinghai for the past 16 ka (Hou et al., 2016). **(D)** Pollen-based T_{ann} (mean annual temperature) from Lake Ximen Cuo on the northeastern TP (Herzschuh et al., 2014). **(E)** Pollen-based P_{ann} (mean annual precipitation) from Lake Ximen Cuo on the northeastern TP (Herzschuh et al., 2014). **(F)** Arctic sea ice extent (de Vernal et al., 2013).

(2014), The excessively humid climate did not favor C_4 plant growth; thus, the $\delta^{13}C_{31}$ value was depleted, representing a decrease in C_4 plant biomass (**Figures 5A,C**). Afterward, the higher $\delta^{18}O_{carb}$ values during 6.2–4.8 cal kyr BP suggest a gradual drying climate, which is beneficial to the growth and expansion of C_4 plants, as reflected by the enriched $\delta^{13}C_{31}$ value (**Figures 5A,C**). The changes in precipitated carbonate $\delta^{18}O$ of the HL05-2 core (**Figure 6B**) (Zhao et al., 2010) and Genggahai Lake (**Figure 7A**) (Qiang et al., 2017) were consistent with the $\delta^{18}O_{carb}$ of the Hl18-3core during this period (**Figure 6B**) (Zhao et al., 2010).

Late Holocene (Ca. 4.8–0.2 cal kyr BP)

In the late Holocene, the $\delta^{18}O_{carb}$ value showed a general depleted trend, similar to that of other climate indices, such as C/N and $\delta^{13}C_{31}$ (**Figures 5A–C**). The $\delta^{18}O_{carb}$ value was enriched during 4.8–4.3 cal kyr BP, while $\delta^{13}C_{31}$ decreased rapidly, indicating a contraction of C_4 plants. All of these proxies signified a strong abrupt cold-dry event (**Figures 5A,C**). The temperature indicator $U^{k'}_{37}$-derived ΔT showed low values during 4.9–4.3 cal kyr BP. Moreover, the carbonate content declined revealing a low lake level, and a higher salinity appeared at ~4.6 cal kyr BP, suggesting a dry climate (**Figures 6C–E**) (Zhao et al., 2013; Zhao et al., 2010; He et al., 2016). The pollen concentration and organic matter percentage were in low value from ~4.2 to 3.7 cal kyr BP (**Figures 6F,G**) (Zhao et al., 2007; Zhao et al., 2013), which demonstrated a dry and deteriorated climate. These results generally signify a cold-dry event, correlated with a 4.2-cal kyr BP event (Bond et al., 1997; Mischke and Zhang, 2010; Hou et al., 2016). The positive $\delta^{18}O_{carb}$ values observed in the Genggahai Lake during ~5.0–~3.5 cal kyr BP, as well as the decreased precipitation in Ximencuo Lake on northeastern Tibetan Plateau during 4.9–3.8 cal kyr BP, indicated that a hydroclimate was dry, while the temperature in the adjacent area of Hurleg Lake, such as the Qinghai and Ximencuo lakes, decreased dramatically (**Figures 6C,D**) (Herzschuh et al., 2014; Hou et al., 2016). In addition, the sea ice coverage in the Barents Sea increased significantly (**Figure 7F**) (De Vernal et al., 2013), sea surface temperature decreased (Lea et al., 2003), and Greenland ice core $\delta^{18}O$ (Stuiver et al., 1995) notably decreased during this period, indicating a global cold event at ~4.2 cal kyr BP.

After the rapid cold-dry event, the climate conditions improved slightly around 4.2–3.0 cal kyr BP, as shown by a negative $\delta^{18}O_{carb}$ (**Figure 5A**), indicating a higher input of effective precipitation. However, the C/N ratio revealed a higher input of terrestrial plants, while the depleted $\delta^{13}C_{31}$ pointed to less C_4 plants (**Figure 5C**). Here we argued that although the C_4 plants decreased, with the more rapid expansion in C_3 plants, it led to a high value of the C/N ratio. In the meantime, the decrease of C_4 plants also suggests that the climate is gradually turning cold (**Figure 5C**). Subsequently, the climate displayed a generally cold-wet trend, as revealed by $\delta^{18}O_{carb}$, C/N, and $\delta^{13}C_{31}$ (**Figures 5A–C**). Fan et al. (2014) reported that a high lake level occurred during 2.2–1.4 cal kyr, and Song et al. (2020) also revealed a moderately wet climate after 2.5 cal kyr BP by sediment grain size and $\delta^{13}C$ of authigenic carbonate in the Hurleg Lake.

Implications Between EASM-Westerly Interaction and Climate Changes

Multiple climate systems including the EASM, the Indian Summer Monsoon (ISM), and the westerly jet (Chen et al., 2008; An et al., 2012; Hou et al., 2017) together contributed to the complex climate condition of the Tibetan Plateau. The Hurleg Lake region now is located outside of the northern edge of the EASM (**Figure 1A**), deduced from the stable isotope analysis of local precipitation collected nearby the Delingha station located ~30 km northeast of the lake (Tian et al., 2001, 2003). The region is located in the transition zone between the westerlies and the EASM, and owing to the instability of the transition zone between the westerly jet and the EASM, the Hurleg Lake area was influenced by both the westerlies and the EASM in the past (Bryson, 1986; Winkler and Wang, 1993; Zhao et al., 2007). However, in contrast to the acknowledged synchronous variation between precipitation and temperature (Zhang et al., 2011) controlled by the EASM, regimes dominated by the westerly jets are multivariable in moisture and other climate conditions (Chen et al., 2019). Neither our temperature indicator ($\delta^{13}C_{31}$) nor our moisture index ($\delta^{18}O_{carb}$) showed a consistent pattern with EASM intensity (**Figure 8E**) or the westerlies; thus, we assume that both of them affected the study area.

In general, the *n*-alkane-derived $\delta^{13}C_{31}$ values (**Figure 8A**, green line)—the temperature-related proxy—showed a similar trend to that of maximum insolation at 35°N since ~16.1 cal kyr BP (**Figure 8A**, black line), which suggests that the long-term temperature variability was controlled by insolation. However, the variation in humidity in the northeastern TP is much more complex than that of temperature. At ~14.8 cal kyr BP, the westerly index (WI) recorded in Qinghai Lake decreased significantly (**Figure 8C**) (An et al., 2012), while the Asian monsoon intensified gradually (**Figure 8E**) (Dykoski et al., 2005). This result coincides with our $\delta^{18}O_{carb}$ values, which suggests that the enriched $\delta^{18}O_{carb}$ at ~14.8 cal kyr BP was caused by the enhanced Asian monsoon. Although we attributed the $\delta^{18}O_{carb}$ variabilities in the HL18-3 core to changes in the Asian monsoon precipitation during 14.8–12.0 cal kyr BP, there may be other controlling factors. We noticed another turning point at ~13.3 cal kyr BP, in which the westerly wind intensified and the Asian monsoon weakened during 13.3–12.0 cal kyr BP. The opposite change occurred during 12.0–11.0 cal kyr BP (**Figures 8C,E**) (An et al., 2012; Dykoski et al., 2005). The negative $\delta^{18}O_{carb}$ value indicates that a wetter climate could have been caused by both the Asian monsoon and westerly wind during 13.3–12.0 cal kyr BP. According to the reconstructed $\delta^{18}O$ and $\delta^{2}H$ values of precipitation in the Qinghai, Bangong Co., and Linggo Co. Lakes in the northern TP, the positive $\delta^{2}H$ values in the three lakes during 10.0–12.0 cal kyr BP support a weakened monsoon in the TP during the late Pleistocene (Yao et al., 2013; Hou et al., 2017). The abrupt decrease in $\delta^{2}H$ in all three lakes during the early Holocene signified an increased monsoon intensity (Yao,

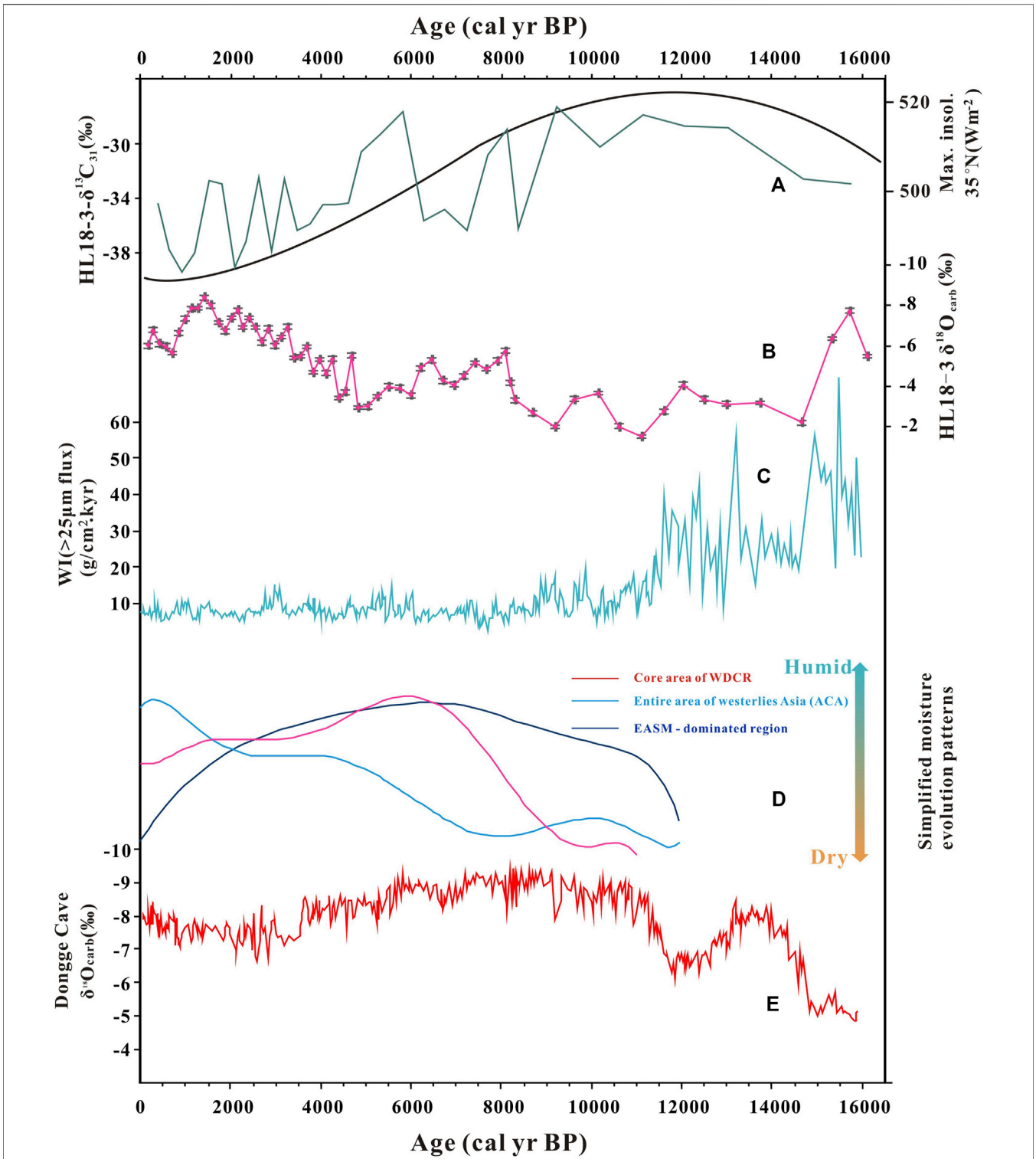

FIGURE 8 | Coordination of the role between EASM and Westerly in the Hurleg lake. **(A)** The $\delta^{13}C_{31}$ in the HL18-3 core (light green), max insolation of 35°N (black line, Laskar et al., 2004). **(B)** The $\delta^{18}O_{carB}$ in the HL18-3 core. **(C)** Lake Qinghai Westerlies climate index (WI, flux of >25 mm fraction) (An et al., 2012). **(D)** Simplified moisture evolution patterns in different regions of Asia during the Holocene (Chen et al., 2019). **(E)** Stalagmite calcite $\delta^{18}O$ from Dongge Cave (Dykoski et al., 2005).

1997; Hou et al., 2017). Thus, it is considered that since ~11 cal kyr BP, the variation of moisture in the Hurleg Lake area was predominantly controlled by Asian monsoon, until ~4.0 cal kyr BP, in which the intensity of monsoon declined gradually (**Figure 8E**) (Dykoski et al., 2005).

Nevertheless, the intensity of the monsoon has been decreasing over the past ~4.0 cal kyr BP (Dykoski et al., 2005), while the depleted $\delta^{18}O_{carb}$ value reflects a wetter climate condition (**Figures 8B,E**). Thus, the Asian monsoon is unlikely to be the dominant moisture source after ~4.0 cal kyr BP, while the synthetic model of humidity from the entire area of westerly Asia (ACA) displayed an increasing trend (**Figure 8D**) (Chen et al., 2019), which likely contributed to the increased humidity in the Hurleg Lake region. Thomas et al. (2016) suggested that the hydroclimate of Qinghai Lake during the late Quaternary was mainly dominated by westerly-derived moisture, and the low $\delta^{18}O_{carb}$ values in the lake during the Little Ice Age was likely caused by westerly-sourced moisture (Henderson et al., 2010). Therefore, the negative shift in the $\delta^{18}O_{carb}$ value during the late Holocene could have resulted from strengthened westerlies, which provided more depleted $\delta^{18}O$ precipitation to the lake (Qiang et al., 2017). The pattern of oxygen isotope fluctuations at Hurleg Lake strongly suggests that the northeastern TP was alternately dominated by the westerlies in the late Holocene.

In summary, the hydroclimatic evolution of Hurleg Lake, as revealed by multiple proxies, including $\delta^{18}O_{carb}$, C/N of HL18-3 core, carbonate content and organic matter percentage (Zhao et al., 2010), and pollen concentration (Zhao et al., 2007), was generally controlled by both the westerlies and the Asian monsoon during the Lateglacial, the Asian monsoon during the early to mid-Holocene, and the westerlies during the late Holocene.

CONCLUSION

Based on multiple geochemical proxies, including inorganic ($\delta^{18}O_{carb}$), and organic indicators (C/N, $\delta^{13}C_{31}$), we reconstructed paleoclimatic evolution history in the Hurleg Lake area, northeastern Tibetan Plateau since ~16.1 cal kyr BP:

1) 16.1–11.1 cal kyr BP (late glacial): a generally warm-wet climate occurred during 16.1–12.0 cal kyr BP, which was interrupted by a cold-dry phase at 12.0–11.1 cal kyr BP.
2) 11.1–4.8 cal kyr BP (early to mid-Holocene): warm-wet climate conditions occurred in the early Holocene, which was interrupted by the 8.3 cal kyr BP cold-dry interval. After then, the climate became wet and warm during the mid-Holocene.
3) 4.8–0.2 cal kyr BP (late Holocene): a cold-dry event occurred during 4.8–4.3 cal kyr BP, which was followed by a cooler climate with increasing humidity.

Comparisons of regional climate records suggest that although several global cold events affected the climate condition of the northeastern TP in the short term, the long-term alternation of cold-warm environmental conditions was controlled by insolation. The hydroclimatic evolution reflected by $\delta^{18}O_{carb}$ documented both westerly and Asian monsoon effective precipitation. By combining multiple hydroclimate proxies, we found that the precipitation in the study region was firstly controlled by both westerly wind and Asian monsoon during the Lateglacial, the Asian monsoon during the early to mid-Holocene, and the westerly winds during the late Holocene.

DATA AVAILABILITY STATEMENT

The original contributions presented in the study are included in the article/Supplementary Material; further inquiries can be directed to the corresponding authors.

AUTHOR CONTRIBUTIONS

XM: participation in the whole work; drafting of the article; ZW: perception and design; YW, GW, and QF: perception and design; final approval of the version to be published; TZ, HM, XY, PZ, JW, and SL: data analysis.

FUNDING

This work was financially supported by the National Key R&D Program of China (Grant No. 2017YFA0604803), the National Natural Science Foundation of China (Grant Nos. 41831176, 41972030, 41902028, and 42072038), the Chinese Academy of Sciences Key Project (Grant No. XDB26020302), and the CAS "Light of West China" Program and the Key Laboratory Project of Gansu (Grant No. 1309RTSA041).

REFERENCES

Alley, R. B., Mayewski, P. A., Sowers, T., Stuiver, M., Taylor, K. C., and Clark, P. U. (1997). Holocene Climatic Instability: a Prominent, Widespread Event 8200 Yr Ago. *Geol* 25, 483–486. doi:10.1130/0091-7613(1997)025<0483:hciapw>2.3.co;2

An, Z., Colman, S. M., Zhou, W., Li, X., Brown, E. T., Jull, A. J. T., et al. (2012). Interplay between the Westerlies and Asian Monsoon Recorded in Lake Qinghai Sediments since 32 Ka. *Sci. Rep.* 2, 619. doi:10.1038/srep00619

Apolinarska, K., and Hammarlund, D. (2009). Multi-component Stable Isotope Records from Late Weichselian and Early Holocene lake Sediments at Imiołki, Poland: Palaeoclimatic and Methodological Implications. *J. Quat. Sci.* 24, 948–959. doi:10.1002/jqs.1274

Araguás-Araguás, L., Froehlich, K., and Rozanski, K. (1998). Stable Isotope Composition of Precipitation over Southeast Asia. *J. Geophys. Res.* 103, 28721–28742. doi:10.1029/98jd02582

Bard, E., Rostek, F., Turon, J.-L., and Gendreau, S. (2000). Hydrological Impact of Heinrich Events in the Subtropical Northeast Atlantic. *Science* 289, 1321–1324. doi:10.1126/science.289.5483.1321

Blaauw, M., Christen, A. J., Vazquez, E. J., Belding, T., Theiler, J., and Gough, B. (2020). Rbacon: Age Depth Modelling Using Bayesian Statistics. R package version 2.4.0. Available at: https://CRAN.R-project.org/package=rbacon.

Blaauw, M., and Christen, J. A. (2011). Flexible Paleoclimate Age-Depth Models Using an Autoregressive Gamma Process. *Bayesian Anal.* 6, 457–474. doi:10.1214/ba/1339616472

Bond, G., Showers, W., Cheseby, M., Lotti, R., Almasi, P., deMenocal, P., et al. (1997). A Pervasive Millennial-Scale Cycle in North Atlantic Holocene and Glacial Climates. *Science* 278, 1257–1266. doi:10.1126/science.278.5341.1257

Bowen, R. (1990). *Isotope and Climates*. Elsevier Applied Science. Science, 96–100.

Bryson, R. A. (1986). "Airstream Climatology of Asia," in Proceedings of International Symposium on the Qinghai-Xizang Plateau and Mountain Meteorology (Boston, MA: American Meteorological Society), 604–619. doi:10.1007/978-1-935704-19-5_36

Cerling, T. E., Harris, J. M., Macfadden, B. J., Leakey, M. G., Quadek, J., Eisenmann, V., et al. (1997). Global Vegetation Change through the Miocene/Pliocene Boundary. *Nature* 1997, 389. doi:10.1038/38229

Chen, F. H., Chen, J. H., Huang, W., Chen, S. Q., Huang, X. Z., Jin, L. J., et al. (2019). Westerlies Asia and Monsoonal Asia: Spatiotemporal Differences in Climate Change and Possible Mechanisms on Decadal to Sub-orbital Timescales. *Earth-Science Rev.* 192, 337–354. doi:10.1016/j.earscirev.2019.03.005

Chen, F., Wu, D., Chen, J., Zhou, A., Yu, J., Shen, J., et al. (2016). Holocene Moisture and East Asian Summer Monsoon Evolution in the Northeastern Tibetan Plateau Recorded by lake Qinghai and its Environs: a Review of Conflicting Proxies. *Quat. Sci. Rev.* 154, 111–129. doi:10.1016/j.quascirev.2016.10.021

Chen, F., Yu, Z., Yang, M., Ito, E., Wang, S., Madsen, D. B., et al. (2008). Holocene Moisture Evolution in Arid central Asia and its Out-of-phase Relationship with Asian Monsoon History. *Quat. Sci. Rev.* 27, 351–364. doi:10.1016/j.quascirev.2007.10.017

Chen, Z., Ma, H. Z., Cao, G. C., Zhang, X. Y., Zhou, D. J., Yao, Y., et al. (2007). Climatic-environmental Evolution in Gahai Lake Area since the Late Glacial Period from Loss-On-Ignition. *Mar. Geology. Quat. Geology.* 27, 131–138. (in chinses with English abstract).

Clegg, B. F., and Hu, F. S. (2010). An Oxygen-Isotope Record of Holocene Climate Change in the South-central Brooks Range, Alaska. *Quat. Sci. Rev.* 29, 928–939. doi:10.1016/j.quascirev.2009.12.009

Dansgaard, W. (1964). Stable Isotopes in Precipitation. *Tellus* 16, 436–468. doi:10.3402/tellusa.v16i4.8993

Dayem, K. E., Molnar, P., Battisti, D. S., and Roe, G. H. (2010). Lessons Learned from Oxygen Isotopes in Modern Precipitation Applied to Interpretation of Speleothem Records of Paleoclimate from Eastern Asia. *Earth Planet. Sci. Lett.* 295, 219–230. doi:10.1016/j.epsl.2010.04.003

De Vernal, A., Hillaire-Marcel, C., Rochon, A., Fréchette, B., Henry, M., Solignac, S., et al. (2013). Dinocyst-based Reconstructions of Sea Ice Cover Concentration during the Holocene in the Arctic Ocean, the Northern north Atlantic Ocean and its Adjacent Seas. *Quat. Sci. Rev.* 79, 111–121. doi:10.1016/j.quascirev.2013.07.006

Develle, A.-L., Herreros, J., Vidal, L., Sursock, A., and Gasse, F. (2010). Controlling Factors on a Paleo-lake Oxygen Isotope Record (Yammoûneh, Lebanon) since the Last Glacial Maximum. *Quat. Sci. Rev.* 29, 865–886. doi:10.1016/j.quascirev.2009.12.005

Diffenbaugh, N. S., Scherer, M., and Ashfaq, M. (2013). Response of Snow-dependent Hydrologic Extremes to Continued Global Warming. *Nat. Clim Change* 3, 379–384370. doi:10.1038/nclimate1732

Dykoski, C., Edwards, R., Cheng, H., Yuan, D., Cai, Y., Zhang, M., et al. (2005). A High-Resolution, Absolute-Dated Holocene and Deglacial Asian Monsoon Record from Dongge Cave, China. *Earth Planet. Sci. Lett.* 233, 71–86. doi:10.1016/j.epsl.2005.01.036

Edwards, E. J., and Smith, S. A. (2010). Phylogenetic Analyses Reveal the Shady History of C4 Grasses. *Proc. Natl. Acad. Sci.* 107, 2532–2537. doi:10.1073/pnas.0909672107

Epstein, S., Buchsbaum, R., Lowenstam, H. A., and Urey, H. C. (1953). Revised Carbonate-Water Isotopic Temperature Scale. *Geol. Soc. America Bull.* 64, 1315–1326. doi:10.1130/0016-7606(1953)64[1315:rcits]2.0.co;2

Fan, Q., Ma, H., Wei, H., and An, F. (2014). Holocene lake-level Changes of Hurleg lake on Northeastern Qinghai-Tibetan Plateau and Possible Forcing Mechanism. *The Holocene* 24, 274–283. doi:10.1177/0959683613517399

Fu, Y., Xiao, J. S., and Xiao, R. X. (2008). Impact of Climate Change on Water Resources in the Qaidam Basin - A Case Study in the Hurleg Lake Basin. *J. Glaciology* 30, 998–1006.

Gao, Y. X. (1962). "On Some Problems of Asian Monsoon," in *Some Questions about the East Asian Monsoon*. Editor Y. X. Gao (Beijing: Chinese Science Press), 1–49. (in Chinese).

Gasse, F., Arnold, M., Fontes, J. C., Fort, M., Gibert, E., Huc, A., et al. (1991). A 13,000-year Climate Record from Western Tibet. *Nature* 353, 742–745. doi:10.1038/353742a0

Günther, F., Witt, R., Schouten, S., Mäusbacher, R., Daut, G., Zhu, L., et al. (2015). Quaternary Ecological Responses and Impacts of the Indian Ocean Summer Monsoon at Nam Co, Southern Tibetan Plateau. *Quat. Sci. Rev.* 112, 66–77. doi:10.1016/j.quascirev.2015.01.023

Haug, G. H., Gunther, D., Peterson, L. C., Sigman, D. M., Hughen, K. A., and Aeschlimann, B. (2003). Climate and the Collapse of Maya Civilization. *Science* 299, 1731–1735. doi:10.1126/science.1080444

He, Y., Zhao, C., Liu, Z., Wang, H., Liu, W., Yu, Z., et al. (2016). Holocene Climate Controls on Water Isotopic Variations on the Northeastern Tibetan Plateau. *Chem. Geology.* 440, 239–247. doi:10.1016/j.chemgeo.2016.07.024

Hede, M. U., Rasmussen, P., Noe-Nygaard, N., Clarke, A. L., Vinebrooke, R. D., and Olsen, J. (2010). Multiproxy Evidence for Terrestrial and Aquatic Ecosystem Responses during the 8.2 Ka Cold Event as Recorded at Højby Sø, Denmark. *Quat. Res.* 73, 485–496. doi:10.1016/j.yqres.2009.12.002

Hedges, J. I., Keil, R. G., and Benner, R. (1997). What Happens to Terrestrial Organic Matter in the Ocean. *Org. Geochem.* 27, 195–212. doi:10.1016/s0146-6380(97)00066-1

Henderson, A. C. G., Holmes, J. A., and Leng, M. J. (2010). Late Holocene Isotope Hydrology of Lake Qinghai, NE Tibetan Plateau: Effective Moisture Variability and Atmospheric Circulation Changes. *Quat. Sci. Rev.* 29, 2215–2223. doi:10.1016/j.quascirev.2010.05.019

Herzschuh, U., Borkowski, J., Schewe, J., Mischke, S., and Tian, F. (2014). Moisture-advection Feedback Supports strong Early-To-Mid Holocene Monsoon Climate on the Eastern Tibetan Plateau as Inferred from a Pollen-Based Reconstruction. *Palaeogeogr. Palaeoclimatol. Palaeoecol.* 402, 44–54. doi:10.1016/j.palaeo.2014.02.022

Herzschuh, U., Winter, K., Wünnemann, B., and Li, S. (2006). A General Cooling Trend on the central Tibetan Plateau throughout the Holocene Recorded by the Lake Zigetang Pollen Spectra. *Quat. Int.* 154-155, 113–121. doi:10.1016/j.quaint.2006.02.005

Hou, J., D'Andrea, W. J., Wang, M., He, Y., and Liang, J. (2017). Influence of the Indian Monsoon and the Subtropical Jet on Climate Change on the Tibetan Plateau since the Late Pleistocene. *Quat. Sci. Rev.* 163, 84–94. doi:10.1016/j.quascirev.2017.03.013

Hou, J., Huang, Y., Zhao, J., Liu, Z., Colman, S., and An, Z. (2016). Large Holocene Summer Temperature Oscillations and Impact on the Peopling of the Northeastern Tibetan Plateau. *Geophys. Res. Lett.* 43, 1323–1330. doi:10.1002/2015gl067317

Hu, L., Guo, Z., Feng, J., Yang, Z., and Fang, M. (2009). Distributions and Sources of Bulk Organic Matter and Aliphatic Hydrocarbons in Surface Sediments of the Bohai Sea, China. *Mar. Chem.* 113, 197–211. doi:10.1016/j.marchem.2009.02.001

Huang, Q., and Cai, B. Q. (1984). "Geochronological Study on the Sediments in Qarhan Lake," in *Proceedings of the Sinl-Australian Quaternary Meeting* (Nanjing: Quaternary Science Committee of China), 106–114. (in Chinese).

IPCC (2014). "Climate Change 2014: Synthesis Report. Contribution of Working Groups I, II and III to the Fifth Assessment Report of the Intergovernmental Panel on Climate Change," in *Core Writing Team*. Editors R. K. Pachauri and L. A. Meyer (Geneva, Switzerland: IPCC), 151.

Jia, G.-D., and Peng, P.-A. (2003). Temporal and Spatial Variations in Signatures of Sedimented Organic Matter in Lingding Bay (Pearl Estuary), Southern China. *Mar. Chem.* 82, 47–54. doi:10.1016/s0304-4203(03)00050-1

Jiang, J. M., and Wu, J. L. (2003). Lake Sediment Records of the Holocene Environmental Evolution in North Xinjiang. *Geol. J. China Universities* 9, 30–37. (In Chinese with English abstract).

Johnsen, S. J., Clausen, H. B., Dansgaard, W., Fuhrer, K., Gundestrup, N., Hammer, C. U., et al. (1992). Irregular Glacial Interstadials Recorded in a New Greenland Ice Core. *Nature* 359, 311–313. doi:10.1038/359311a0

Johnson, K. R., and Ingram, B. L. (2004). Spatial and Temporal Variability in the Stable Isotope Systematics of Modern Precipitation in China: Implications for

Paleoclimate Reconstructions. *Earth Planet. Sci. Lett.* 220, 365–377. doi:10.1016/s0012-821x(04)00036-6

Klanderud, K. (2005). Climate Change Effects on Species Interactions in an alpine Plant Community. *J. Ecol.* 93, 127–137. doi:10.1111/j.1365-2745.2004.00944.x

Kramer, A., Herzschuh, U., Mischke, S., and Zhang, C. (2010). Late Glacial Vegetation and Climate Oscillations on the southeastern Tibetan Plateau Inferred from the Lake Naleng Pollen Profile. *Quat. Res.* 73, 324–335. doi:10.1016/j.yqres.2009.12.003

Leng, M. J., and Marshall, J. D. (2004). Palaeoclimate Interpretation of Stable Isotope Data from lake Sediment Archives. *Quat. Sci. Rev.* 23, 811–831. level of tropical lakes. Nature. 317, 130–134. doi:10.1016/j.quascirev.2003.06.012

Lister, G. S., Kelts, K., Zaoc, C. K., Yua, J.-K., and Niessena, F. (1991). Lake Qinghai, China: Closed-basin lake levels and the oxygen isotope record for ostracoda since the latest Pleistocene. *Palaeogeo. Palaeoclim. Palaeoecol.* 84, 141–162.

Liu, H., and Liu, W. (2016). *n*-Alkane Distributions and Concentrations in Algae, Submerged Plants and Terrestrial Plants from the Qinghai-Tibetan Plateau. *Org. Geochem.* 99, 10–22. doi:10.1016/j.orggeochem.2016.06.003

Liu, W., Yang, H., Wang, H., An, Z., Wang, Z., and Leng, Q. (2015). Carbon Isotope Composition of Long Chain Leaf Wax N -alkanes in lake Sediments: A Dual Indicator of Paleoenvironment in the Qinghai-Tibet Plateau. *Org. Geochem.* 83-84, 190–201. doi:10.1016/j.orggeochem.2015.03.017

Liu, X., and Chen, B. (2000). Climatic Warming in the Tibetan Plateau during Recent Decades. *Int. J. Climatol.* 20, 1729–1742. doi:10.1002/1097-0088(20001130)20:14<1729::aid-joc556>3.0.co;2-y

Liu, X., Cheng, Z., Yan, L., and Yin, Z.-Y. (2009). Elevation Dependency of Recent and Future Minimum Surface Air Temperature Trends in the Tibetan Plateau and its Surroundings. *Glob. Planet. Change* 68, 164–174. doi:10.1016/j.gloplacha.2009.03.017

Liu, X., Shen, J., Wang, S., Wang, Y., and Liu, W. (2007). Southwest Monsoon Changes Indicated by Oxygen Isotope of Ostracode Shells from Sediments in Qinghai Lake Since the Late Glacial. *Chin. Sci. Bull.* 52, 539–544.

Lunt, D. J., Elderfield, H., Pancost, R., Ridgwell, A., Foster, G. L., Haywood, A., et al. (2013). Warm Climates of the Past-Aa Lesson for the Future. *Philos. Trans. A. Math. Phys. Eng. Sci.* 371, 20130146. doi:10.1098/rsta.2013.0146

Ma, H., Wang, Y.-L., Jin, C.-S., Wei, Z.-F., Wang, G., Zhang, T., et al. (2021). Relative Paleointensity Correction of Radiocarbon Reservoir Effect for Lacustrine Sediments on the Northeast Tibetan Plateau. *Quat. Geochronol.* 65, 101193. doi:10.1016/j.quageo.2021.101193

Ma, X. Y., Wei, Z. F., Wang, Y. L., Wang, G., Zhang, T., Ma, H., et al. (2021a). *Insolation and Seasonal Differences Affecting C_3 vs C_4 Plant Abundance since the Late Deglacial on the Northeastern Tibetan Plateau*. submitted for publication.

Meyers, P. A. (1997). Organic Geochemical Proxies of Paleoceanographic, Paleolimnologic, and Paleoclimatic Processes. *Org. Geochem.* 27, 213–250. doi:10.1016/s0146-6380(97)00049-1

Meyers, P. A. (1994b). Preservation of Elemental and Isotopic Source Identification of Sedimentary Organic Matter. *Chem. Geology.* 114, 289–302. doi:10.1016/0009-2541(94)90059-0

Mischke, S., Weynell, M., Zhang, C., and Wiechert, U. (2013). Spatial Variability of 14C Reservoir Effects in Tibetan Plateau Lakes. *Quat. Int.* 313-314, 147–155. doi:10.1016/j.quaint.2013.01.030

Mischke, S., and Zhang, C. (2010). Holocene Cold Events on the Tibetan Plateau. *Glob. Planet. Change* 72, 155–163. doi:10.1016/j.gloplacha.2010.02.001

Mondoni, A., Rossi, G., Orsenigo, S., and Probert, R. J. (2012). Climate Warming Could Shift the Timing of Seed Germination in alpine Plants. *Ann. Botlondon* 110, 155–164. doi:10.1093/aob/mcs097

Peterse, F., Martínez-García Alfredo, Z. B., Beets, C. J., Prins, M. A., Zheng, H., et al. (2004). Molecular Records of continental Air Temperature and Monsoon Precipitation Variability in East Asia Spanning the Past 130,000 Years. *Quat. Sci. Rev.* 83, 76–82.

Peterse, F., Prins, M. A., Beets, C. J., Troelstra, S. R., Zheng, H., Gu, Z., et al. (2011). Decoupled Warming and Monsoon Precipitation in East Asia over the Last Deglaciation. *Earth Planet. Sci. Lett.* 301, 256–264. doi:10.1016/j.epsl.2010.11.010

Qiang, M. R. (2002). "Holocene Climatic Changes Documented by Sediments from Sugan Lake in the Qaidam Basin, Northern Tibetan Plateau, China." PhD Dissertation. Gaithersburg, MD: Lanzhou Univeristy. (in Chinese).

Qiang, M., Song, L., Jin, Y., Li, Y., Liu, L., Zhang, J., et al. (2017). A 16-ka Oxygen-Isotope Record from Genggahai Lake on the Northeastern Qinghai-Tibetan Plateau: Hydroclimatic Evolution and Changes in Atmospheric Circulation. *Quat. Sci. Rev.* 162, 72–87. doi:10.1016/j.quascirev.2017.03.004

Rao, Z., Jia, G., Qiang, M., and Zhao, Y. (2014). Assessment of the Difference between Mid- and Long Chain Compound Specific δDn-alkanes Values in Lacustrine Sediments as a Paleoclimatic Indicator. *Org. Geochem.* 76, 104–117. doi:10.1016/j.orggeochem.2014.07.015

Reimer, P. J., Bard, E., Bayliss, A., Beck, J. W., Blackwell, P. G., Ramsey, C. B., et al. (2013). IntCal13 and Marine13 Radiocarbon Age Calibration Curves 0-50,000 Years Cal BP. *Radiocarbon* 55, 1869–1887. doi:10.2458/azu_js_rc.55.16947

Reimer, R., and Reimer, P. (2006). Marine Reservoir Corrections and the Calibration Curve. *PAGES news* 14, 12–13. doi:10.22498/pages.14.3.12

Rieley, G., Collister, J. W., Stern, B., and Eglinton, G. (1993). Gas Chromatography/isotope Ratio Mass Spectrometry of Leaf Wax N-Alkalines from Plants of Differing Carbon Dioxide Metabolisms. *Rapid Commun. Mass. Spectrom.* 7, 488–491. doi:10.1002/rcm.1290070617

Schneider, L., Pain, C. F., Haberle, S., Blong, R., Alloway, B. V., Fallon, S. J., et al. (2019). Evaluating the Radiocarbon Reservoir Effect in lake Kutubu, papua new guinea. *Radiocarbon* 61, 287–308. doi:10.1017/rdc.2018.49

Song, G., Wang, H., and Shi, L. (2020). Climate Evolution since 9.32 Cal Ka BP in Keluke lake, Northeastern Qaidam Basin, China. *J. Arid Environments* 178, 104149. doi:10.1016/j.jaridenv.2020.104149

Soulet, G., Giosan, L., Flaux, C., and Galy, V. (2019). Using Stable Carbon Isotopes to Quantify Radiocarbon Reservoir Age Offsets in the Coastal Black Sea. *Radiocarbon* 61, 309–318. doi:10.1017/rdc.2018.61

Strömberg, C. A. E. (2011). Evolution of Grasses and Grassland Ecosystems. *Annu. Rev. Earth Planet. Sci.* 39, 517–544. doi:10.1146/annurev-earth-040809-152402

Stuiver, M., Grootes, P. M., and Braziunas, T. F. (1995). The GISP2 δ18O Climate Record of the Past 16,500 Years and the Role of the Sun, Ocean, and Volcanoes. *Quat. Res.* 44, 341–354. doi:10.1006/qres.1995.1079

Talbot, M. R. (1990). A Review of the Palaeohydrological Interpretation of Carbon and Oxygen Isotopic Ratios in Primary Lacustrine Carbonates. *Chem. Geology. Isotope Geosci. section* 80, 261–279. doi:10.1016/0168-9622(90)90009-2

Talbot, M. R., and Livingstone, D. A. (1989). Hydrogen index and Carbon Isotopes of Lacustrine Organic Matter as lake Level Indicators. *Palaeogeogr. Palaeoclimatol. Palaeoecol.* 70, 121–137. doi:10.1016/0031-0182(89)90084-9

Thomas, E. K., Huang, Y., Clemens, S. C., Colman, S. M., Morrill, C., Wegener, P., et al. (2016). Changes in Dominant Moisture Sources and the Consequences for Hydroclimate on the Northeastern Tibetan Plateau during the Past 32 Kyr. *Quat. Sci. Rev.* 131, 157–167. doi:10.1016/j.quascirev.2015.11.003

Thomas, E. R., Wolff, E. W., Mulvaney, R., Steffensen, J. P., Johnsen, S. J., Arrowsmith, C., et al. (2007). The 8.2ka Event from Greenland Ice Cores. *Quat. Sci. Rev.* 26, 70–81. doi:10.1016/j.quascirev.2006.07.017

Tian, L., Liu, Z., Gong, T., Yin, C., Yu, W., and Yao, T. (2008). Isotopic Variation in the lake Water Balance at the Yamdruk-Tso basin, Southern Tibetan Plateau. *Hydrol. Process.* 22, 3386–3392. doi:10.1002/hyp.6919

Tian, L., Masson-Delmotte, V., Stievenard, M., Yao, T., and Jouzel, J. (2001). Tibetan Plateau Summer Monsoon Northward Extent Revealed by Measurements of Water Stable Isotopes. *J. Geophys. Res.* 106, 28018–28088. doi:10.1029/2001jd900186

Tian, L., Yao, T., MacClune, K., White, J. W. C., Schilla, A., Vaughn, B., et al. (2007). Stable Isotopic Variations in West China: a Consideration of Moisture Sources. *J. Geophys. Res.* 112, D10112. doi:10.1029/2006jd007718

Tian, L., Yao, T., Schuster, P. F., White, J. W. C., Ichiyanagi, K., Pendall, E., et al. (2003). Oxygen-18 Concentrations in Recent Precipitation and Ice Cores on the Tibetan Plateau. *J. Geophys. Res.* 108 (D9), a–n. doi:10.1029/2002JD002173

Tierney, J. E., Poulsen, C. J., Montañez, I. P., Bhattacharya, T., Feng, R., Ford, H. L., et al. (2020). Past Climates Inform Our Future. *Science* 370 (6517), eaay3701. doi:10.1126/science.aay3701

Wang, G., Wang, Y., Wei, Z., He, W., Zhang, T., and Ma, X. (2020). Geochemical Records of Qionghai Lake Sediments in Southwestern China Linked to Late Quaternary Climate Changes. *Palaeogeogr. Palaeoclimatol. Palaeoecol.* 560, 109902. doi:10.1016/j.palaeo.2020.109902

Wang, S. M., and Dou, H. S. (1998). *Lakes in China*. Beijing: Science Press. (in Chinese).

Wang, Y., Cheng, H., Edwards, R. L., He, Y., Kong, X., An, Z., et al. (2005). The Holocene Asian Monsoon: Links to Solar Changes and north Atlantic Climate. *Science* 308, 854–857. doi:10.1126/science.1106296

Wang, Y., Cheng, H., Edwards, R. L., Kong, X., Shao, X., Chen, S., et al. (2008). Millennial- and Orbital-Scale Changes in the East Asian Monsoon over the Past 224,000 Years. *Nature* 451, 1090–1093. doi:10.1038/nature06692

Wei, K., and Gasse, F. (1999). Oxygen Isotopes in Lacustrine Carbonates of Western China Revisited: Implications for Post Glacial Changes in Summer Monsoon Circulation. *Quat. Sci. Rev.* 18, 1315–1334.

Winkler, M. G., and Wang, P. K. (1993). "The Late-Quaternary Vegetation and Climate of China," in *Global Climates since the Last Glacial Maximum*. Editors H. E. Wright, J. E. Kutzbach, T. WebbIII, W. F. Ruddiman, F. A. Street-Perrott, and P. J. Bartlein (Minneapolis, MN: University of Minnesota Press), 221–264.

Xiao, J., Xu, Q., Nakamura, T., Yang, X., Liang, W., and Inouchi, Y. (2004). Holocene Vegetation Variation in the Daihai Lake Region of north-central China: a Direct Indication of the Asian Monsoon Climatic History. *Quat. Sci. Rev.* 23, 1669–1679. doi:10.1016/j.quascirev.2004.01.005

Yao, T. D. (1997). Climatic and Environmental Record in the Past about 2000 Years from the Guliya Ice Core. *Quat. Sci.* 1, 52–59. (In Chinese with English abstract).

Yao, T., Masson-Delmotte, V., Gao, J., Yu, W., Yang, X., Risi, C., et al. (2013). A Review of Climatic Controls on δ18O in Precipitation over the Tibetan Plateau: Observations and Simulations. *Rev. Geophys.* 51, 525–548. doi:10.1002/rog.20023

Yi, X., Yang, D., and Xu, W. (1992). *China Regional Hydrogeology Survey Report-Toson Lake Map (J-47- [25]) 1:200,000Qaidam Integrative Geology Survey*. Golmud, Qinghai, China.

Yu, Z., and Eicher, U. (1998). Abrupt Climate Oscillations during the Last Deglaciation in central North America. *Science* 282, 2235–2238. doi:10.1126/science.282.5397.2235

Zhang, C. J., Zhang, W. Q., Zhang, L., Wang, X. Y., and Berthe, I. (2016). The Characteristics of Carbon and Oxygen Isotopes of Carbonates and Carbon Isotopes of Organic Matter of Bulk Sediments and Their Responses to lake Environments in Western and Northeastern china. *Bull. Mineralogy, Pet. Geochem.* 35, 609–617. (In Chinese with English abstract).

Zhang, C., and Mischke, S. (2009). A Lateglacial and Holocene lake Record from the Nianbaoyeze Mountains and Inferences of lake, Glacier and Climate Evolution on the Eastern Tibetan Plateau. *Quat. Sci. Rev.* 28, 1970–1983. doi:10.1016/j.quascirev.2009.03.007

Zhang, J., Chen, F., Holmes, J. A., Li, H., Guo, X., Wang, J., et al. (2011). Holocene Monsoon Climate Documented by Oxygen and Carbon Isotopes from lake Sediments and Peat Bogs in china: a Review and Synthesis. *Quat. Sci. Rev.* 30, 1973–1987. doi:10.1016/j.quascirev.2011.04.023

Zhang, J., Ma, X., Qiang, M., Huang, X., Li, S., Guo, X., et al. (2016a). Developing Inorganic Carbon-Based Radiocarbon Chronologies for Holocene lake Sediments in Arid NW China. *Quat. Sci. Rev.* 144, 66–82. doi:10.1016/j.quascirev.2016.05.034

Zhao, C., Liu, Z., Rohling, E. J., Yu, Z., Liu, W., He, Y., et al. (2013). Holocene Temperature Fluctuations in the Northern Tibetan Plateau. *Quat. Res.* 80, 55–65. doi:10.1016/j.yqres.2013.05.001

Zhao, C., Yu, Z., Zhao, Y., and Ito, E. (2009). Possible orographic and solar controls of late holocene centennial-scale moisture oscillations in the northeastern tibetan plateau. *Geophys. Res. Lett.* 36(21).

Zhao, C., Yu, Z., Zhao, Y., Ito, E., Kodama, K. P., and Chen, F. (2010). Holocene Millennial-Scale Climate Variations Documented by Multiple lake-level Proxies in Sediment Cores from Hurleg Lake, Northwest china. *J. Paleolimnol* 44, 995–1008. doi:10.1007/s10933-010-9469-6

Zhao, Y., Yu, Z., Chen, F., Ito, E., and Zhao, C. (2007). Holocene Vegetation and Climate History at Hurleg Lake in the Qaidam Basin, Northwest China. *Rev. Palaeobotany Palynology* 145, 275–288. doi:10.1016/j.revpalbo.2006.12.002

Zhao, Y., Yu, Z., and Zhao, W. (2011). Holocene vegetation and climate histories in the eastern Tibetan Plateau: controls by insolation-driven temperature or monsoon-derived precipitation changes. *Quaternary Science Reviews* 30, 1173–1184. doi:10.1016/j.quascirev.2011.02.006

Zhou, L. H., Sun, S. Z., and Chen, G. C. (1990). *Vegetation of Qinghai Province (1:1,000,000)*. Beijing: China Science and Technology Press, 23–24. (in Chinese).

Zhou, W., Cheng, P., Jull, A. J. T., Lu, X., An, Z., Wang, H., Zhu, Y., and Wu, Z. (2014). 14C Chronostratigraphy for Qinghai Lake in China. *Radiocarbon* 56, 143–155. doi:10.2458/56.16470

Conflict of Interest: The authors declare that the research was conducted in the absence of any commercial or financial relationships that could be construed as a potential conflict of interest.

Publisher's Note: All claims expressed in this article are solely those of the authors and do not necessarily represent those of their affiliated organizations, or those of the publisher, the editors, and the reviewers. Any product that may be evaluated in this article, or claim that may be made by its manufacturer, is not guaranteed or endorsed by the publisher.